Air Pollution Science for the 21st Century
J. Austin, P. Brimblecombe and W. Sturges, editors

Chapter 18

Formation and cycling of aerosols in the global troposphere

Frank Raes, Rita Van Dingenen, Elisabetta Vignati, Julian Wilson, Jean-Philippe Putaud

Environment Institute, European Commission, 21020 Ispra (VA), Italy
E-mail: frank.raes@jrc.it

John H. Seinfeld, Peter Adams

California Institute of Technology, Pasadena, CA, USA

Abstract

Aerosols are formed, evolve, and are eventually removed within the general circulation of the atmosphere. The characteristic time of many of the microphysical aerosol processes is days up to several weeks, hence longer than the residence time of the aerosol within a typical atmospheric compartment (e.g. the marine boundary layer, the free troposphere, etc.). Hence, to understand aerosol properties, one cannot confine the discussion to such compartments, but one needs to view aerosol microphysical phenomena within the context of atmospheric dynamics that connects those compartments. This paper attempts to present an integrated microphysical and dynamical picture of the global tropospheric aerosol system. It does so by reviewing the microphysical processes and those elements of the general circulation that determine the size distribution and chemical composition of the aerosol, and by implementing both types of processes in a diagnostic model, in a 3-D global Chemical Transport Model, and in a General Circulation Model. Initial results are presented regarding the formation, transformation, and cycling of aerosols within the global troposphere.

1. Introduction

Particles in the atmosphere arise from natural sources, such as wind-borne dust, sea spray, and volcanoes, and from anthropogenic activities, such as combustion of fuels (Table 1). Emitted directly as particles (primary aerosol) or formed in the atmosphere by gas-to-particle conversion processes (secondary aerosol),

First published in Atmospheric Environment 34 (2000) 4215–4240

Table 1. Estimated global emission rates of particles into the atmosphere (Tg yr^{-1})

	Source strength (Tg yr^{-1})	Reference
Sea salt		
Total	5900	Tegen et al. (1997)
0–2 μm	82.1	Gong et al. (1997)
2–20 μm	2460	
Soil dust		
< 1 μm	250	Tegen and Fung (1995)
1–10 μm	1000	
0.2–2 μm	250	Penner, personal comm.
2–20 μm	4875	
Organic carbon		
Total	69	Liousse et al. (1996)
Biomass burning	54.3	Penner, personal comm.
Fossil fuel	28.8	
Terpene oxidation	18.5	Griffin et al. (1999)
Black carbon		
Total	12	Liousse et al. (1996)
Biomass burning	5.6	
Fossil fuel	6.6	
Sulfate (as H_2SO_4)		
Total	150	Chin and Jacob (1996)
Natural	32	Koch et al. (1999)
Anthropogenic	111	
Nitrate	11.3[a]	Adams et al. (1999)
Ammonium	33.6	Adams et al. (1999)

[a]Nitrate source strength is based on a computed burden of 0.13 Tg and an assumed lifetime of 4.2 d (same as ammonium).

atmospheric aerosols range in size from a few nanometers (nm) to tens of micrometers (μm) in diameter. Once airborne, particles evolve in size and composition through condensation of vapour species or by evaporation, by coagulating with other particles, by chemical reaction, or by activation in the presence of supersaturated water vapour to become cloud and fog droplets. Particles smaller than 1 μm diameter generally have atmospheric concentrations in the range from 10 to 10,000s per cm^3; those exceeding 1 μm diameter typically exhibit concentrations less than 10 cm^{-3}.

There is evidence that anthropogenic particles, at concentrations typical of urban airsheds, directly affect human health. Biomass burning, especially in the tropics, leads to significant perturbations to tropospheric aerosol loadings in that region, perhaps accompanied by alterations of cloud behaviour. Aircraft

exhaust particles in the upper atmosphere are a source of ice and cloud nuclei. Atmospheric particles provide surfaces for heterogeneous chemical reactions that may influence gas-phase chemistry in the troposphere. It is not possible to survey each of these aspects in a review of modest length; consequently, we focus here on aerosol processes in the global atmosphere, the dynamics that shape the size and composition of the global aerosol.

The first measurements of the aerosol number concentration in the atmosphere were performed by Aitken (1888) who used an expansion chamber to make water vapour condense on the particles and make them grow to visible droplets. Aitken proclaimed that "without aerosols there would be no clouds and no precipitation". The water vapour supersaturation (= relative humidity (%) – 100) created in the Aitken counter reached 300%, enough to activate any particle. In the atmosphere, however, supersaturations of at most 2% are reached (Pruppacher and Klett, 1980), and Köhler (1936) showed that at such low supersaturations only those particles will activate that are sufficiently hygroscopic, i.e. particles that contain sufficient amount of soluble material to reduce the equilibrium water vapour pressure above the solution droplet. Hence, aerosol chemical and physical properties do control cloud droplet formation, and accordingly cloud microphysical properties, precipitation potential and optical properties. There are now many observations that this is effectively the case (Boers et al., 1994; Cerveny and Balling, 1998; Rosenfeld, 1999; Pawlowska and Brenguier, 2000; Johnson et al., 2000; Chuang et al., 2000).

Aerosols are important players in the hydrological cycle and climate system. It is therefore necessary to understand their cycling in the atmosphere, and to be able to predict their characteristics. Within the context of global climate change, aerosol studies have focused either on descriptions of global sources and spatial distributions of aerosols, neglecting the microphysical aspects, or they have focused on the microphysics of their formation and evolution, without placing these processes in the context of atmospheric large-scale circulation. In this paper we will review progress achieved by the two approaches, and we will attempt to synthesise a combined microphysical and dynamical picture of the global tropospheric aerosol system. We will also review observations of some key aerosol characteristics in a number of environments, which have been helpful to constrain our understanding of aerosols. In the model studies, presented at the end of the paper, we draw particularly from the global sulphur cycle because much has been learned recently about this cycle, and it serves as an excellent vehicle to discuss the effect of global circulation on aerosol properties and behaviour.

2. Microphysics of aerosol formation and evolution

2.1. Processes

Fig. 1 depicts generally the microphysical processes that influence the size distribution and chemical composition of the atmospheric aerosol, highlighting the large range of sizes that are involved in the formation and evolution of aerosol particles. Traditionally, atmospheric aerosols have been divided into two size classes: coarse ($D_p > 1$ μm) and fine ($D_p < 1$ μm), reflecting the two major formation mechanisms: primary and secondary. Both populations strongly overlap, however, in the 0.1–1 μm diameter range.

Primary particles that are derived from the break-up and suspension of bulk material by the wind, such as sea salt, soil dust, and biological material, have most of their mass associated with particles of diameters exceeding 1 μm, however, their highest number concentrations occur in the 0.1–1 μm range. For such emission mechanisms, the particle number concentration increases nonlinearly with increasing wind speed (O'Dowd and Smith, 1993; Schulz et al., 1998). Because of their low concentrations and large sizes, primary particles generally do not coagulate with one another, but they can mix with other species through exchange of mass with the gas phase. A particular and impor-

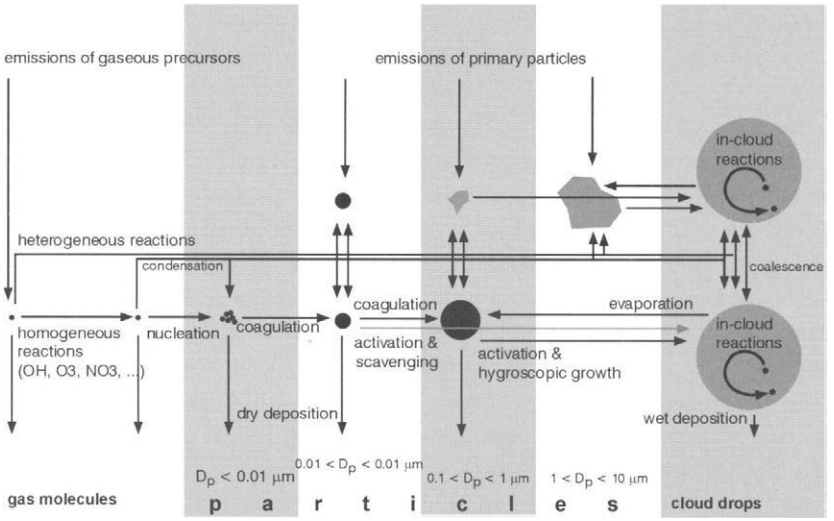

Figure 1. Scheme of the microphysical processes that influence the size distribution and chemical composition of the atmospheric aerosol. The scheme highlights the large range of sizes that are involved in the formation and evolution of aerosol particles, and how aerosols participate in atmospheric chemical processes through homogeneous, heterogeneous and in-cloud reactions.

tant type of primary particles are soot particles formed in combustion. Initially they are formed at high concentrations within the combustion process as particles with a diameter of 5–20 nm. They coagulate however rapidly to form fractal-like aggregates, which, in turn, will collapse to more compact structures of several tens of nanometers due to capillary forces of condensing vapours.

Secondary aerosol mass is formed by transformation of gaseous compounds to the liquid or solid phase. This occurs when the concentration of the compound in the gas phase exceeds its equilibrium vapour pressure above the aerosol surface. In the atmosphere, several processes can lead to such a state of supersaturation:

(1) gas-phase chemical reactions leading to an increase in the gas-phase concentration of compounds with low equilibrium vapour pressure. Examples are:

$$SO_2 + OH \rightarrow \text{(known reaction scheme)} \rightarrow H_2SO_4,$$

$$NO_2 + OH \rightarrow HNO_3,$$

$$\alpha - \text{pinene} + O_3 \rightarrow \text{(unknown reaction scheme)} \rightarrow \text{pinic acid},$$

(2) lowering the ambient temperature leading to a lowering of the equilibrium vapour pressure above the aerosol,

(3) formation of multicomponent aerosol, so that the equilibrium vapour pressure of the single compounds above the aerosol is lowered by the presence of other species in the aerosol (Raoult effect).

The equilibrium vapour pressure over a spherical particle increases with increasing curvature of the particle (Kelvin effect), hence the equilibrium vapour pressure above molecular clusters formed by random collisions is much larger than that above a film on a pre-existing particle or flat surface. Consequently, molecular clusters will generally evaporate. Their growth to a stable size, i.e. nucleation, will be favoured primarily by the absence of pre-existing aerosol surface, and by extreme realisations of the three processes described above. Classical nucleation theory predicts that nucleation is highly nonlinearly dependent on the concentration of the nucleating species in the gas phase.

When nucleation does occur, the new particles grow by condensation and self-coagulation. As particles reach a diameter of the order of the mean free path length of the condensing molecule (typically about 60 nm), condensation becomes diffusion limited and slows down. Also, self-coagulation, which is a second-order process, eventually quenches as number concentrations fall. Hence, under background tropospheric conditions, particles formed initially by nucleation require days to weeks to grow larger than about 0.1 μm solely by condensation and coagulation. Under polluted, urban type conditions, this growth can occur within a day (Raes et al., 1995).

One straightforward way of accumulating secondary aerosol species in the 0.1–1 μm diameter range is by condensation on primary particles emitted in that range. Another more elusive but important growth process is by chemical processing in non-precipitating clouds (Mason, 1971; Friedlander, 1977; Hoppel et al., 1986, 1994a). This process begins with the activation of aerosols, which is the uncontrolled uptake of water once water vapour becomes supersaturated above a certain critical limit. According to traditional Köhler theory, the critical supersaturation for activation depends on the amount of soluble material in the particle and its hygroscopicity, i.e. tendency of the material, once dissolved, to lower the equilibrium water vapour pressure over the solution (Pruppacher and Klett, 1980). The critical supersaturation needed to activate all particles larger than a given dry size increases with decreasing particle size. When the supersaturation in an air parcel rises, cloud activation will therefore preferentially occur on larger particles. The rapid condensation of water quenches a further increase of the supersaturation (which usually does not exceed 2%), so that activation is limited to a subset of particles (cloud condensation nuclei, CCN). For example, for pure ammonium sulphate aerosol and a maximum supersaturation of 0.2%, typical for marine stratus clouds, only particles larger than about 80 nm in diameter will activate. Once a droplet is formed, gaseous species like SO_2 can dissolve and be oxidised in the aqueous phase. When the droplets evaporate, the residue particles are larger than the original CCN upon which the droplets formed as a result of the additional oxidised material, e.g. sulphate from the following aqueous-phase reactions:

$$S(IV) + O_3 \rightarrow S(VI) + O_2,$$

$$S(IV) + H_2O_2 \rightarrow S(VI) + H_2O.$$

Reactions occurring in clouds might also occur in non-activated aerosol solution droplets, however, with different efficiencies because of the larger ionic strength in such droplets. Moreover, some gases might also react on the aerosol surface producing products that might either remain on the particle or return into the gas phase. Examples are the heterogeneous conversion of NO_x to HONO on fresh soot aerosol (Ammann et al., 1998) and halogen release from sea salt (Vogt et al., 1996).

Aerosols are removed from the atmosphere by dry and wet processes. Small particles ($D_p < 1$ μm) diffuse to the Earth's surface, a process which becomes less efficient as the particle size increases. Large particles ($D_p > 1$ μm) settle gravitationally, a process which becomes less efficient as the particle size decreases. In the range $0.1 < D_p < 1$ μm, dry removal is very slow, and the formation and growth processes discussed above tend to accumulate the aerosol

in this size range. These particles, when they have the right hygroscopic properties, will be removed mainly by activation in clouds and subsequent precipitation.

It has become generally accepted to name particles with a diameter in the range $0.1 < D_p < 1$ μm *Accumulation mode particles*, particles in the range $0.01 < D_p < 0.1$ μm *Aitken mode particles*, and particles with $D_p < 0.01$ μm *Nucleation mode particles*. Particles with $D_p > 1$ μm are called *Coarse mode particles*. The idea to represent the aerosol size distribution with a number of log-normally distributed modes is supported by measurements (see Section 3) and was first ventured by Whitby (1978).

Each of the processes in Fig. 1 has a characteristic time. Table 2 presents such times for some of these processes. They are derived in Appenix A con-

Table 2. Aerosol properties and characteristic times of processes in various atmospheric compartments. As the characteristic time the "e-folding time" is used, i.e. the inverse relative rate of change of a property through a process. (See Appendix A)

	Continental boundary layer		Marine boundary layer		Free troposphere	
	Urban	Sub-urban	Polluted	Clean	Clean	Dust
Characteristic time for coagulation with Aitken and accumulation mode, and with clouds (d)						
Nucleation ($D_p = 6$ nm)	0.036	0.095	0.14	1.0	9.4	2.8
Aitken ($D_p = 60$ nm)	0.2	0.7	1.1	7.6	34	11
Accumulation ($D_p = 300$ nm)	1.4	4.8	10	66	754	168
Characteristic time for volume production by condensation (d)						
Nucleation mode	0.5	1.0	2.4	1.5	0.5	
Aitken mode	1.1	2.6	42	11	1.6	94
Accumulation mode	5.0	12	97	52	5.5	206
All aerosol	4.5	12	83	49	4.9	156
Characteristic time for volume production by cloud processing (d)						
Activated aerosol	0.16	0.42	3.0	1.8		
Characteristic time for wet deposition of volume (d)						
All aerosol				0.5–50		
Compartment Properties						
Residence time	1 day	5–10 days	1–2 weeks	1–2 weeks	2–4 weeks	2–4 weeks
SO_2 (pptV)	1000	600	100	20	20	20
fraction SO_4	0.2	0.3	0.5	0.5	0.5	0.5
N_{tot} (/cm^3)	35000	6500	2600	480	300	550
N ($D_p > 80$ nm) (/cm^3)	4520	2695	1866	181	65	186

sidering conditions that are typical for various atmospheric compartments. In order to understand the behaviour of aerosols in a given compartment, it is useful to compare the process characteristic times with the compartment residence times. Loss processes (coagulation, deposition) which occur on a time scale that is small compared to the compartment residence time, indicate an unstable, i.e. decaying, property. Time scales that are long compared to compartment residence times lead to stable properties within the compartment and inter-compartment exchange of those properties. For instance, the extremely short residence time of nucleation mode particles in the boundary layer, due to coagulation with larger particles, implies that they can only be observed in the immediate vicinity of their sources. Hence, as these ultrafine particles are frequently observed in the polluted continental boundary layer (see Fig. 2), the urban and sub-urban continental compartment must contain sources for nucleation mode aerosol. The absence of a persistent nucleation mode in the MBL indicates that in this case no strong in-situ sources for this mode are available. However, occasional nucleation bursts could temporally occur leading to an unstable and rapidly decaying nucleation mode. Because of their short life time, nucleation mode particles are generally not exchanged between the atmospheric compartments, unless they happen at the boundaries of such compartments. Accumulation mode particles on the other hand decay much slower and as such they can travel from one compartment to the other, mixing their properties with the ones of newly formed aerosol within the next compartment.

A comparison of the time scales for condensation and cloud processing show that cloud processing is the major mechanism for growth. Obviously, this applies only for particles that are activated in clouds. In the urban boundary layer, enough condensing material is available to maintain the Aitken mode mass ($\tau_{cond} < \tau_{res}$). When a polluted air mass advects over the ocean, it is cut off

Figure 2. Number (N) and Volume (V) size distributions observed at (a) an urban site (Milan, Italy); (b) a con-urban site (semi-rural area 50 km from Milan, Italy); (c) a marine boundary layer site, 2 days downwind the European continent (Tenerife in the north–east Atlantic); (d) a marine boundary layer site during transport from the open Atlantic (Tenerife); (e) north–east Atlantic lower free troposphere (FT) during background conditions (Tenerife, 2360 m altitude), (f) north–east Atlantic lower free troposphere during African dust transport in the FT (Tenerife, 2360 m altitude). Black lines are data obtained with a differential mobility analyser. Gray lines are data obtained with an optical particle counter (Grimm Dustcheck®) (b), or aerodynamic particle sizer (APS®, TSI Inc.) (c–f), (data not avialable for urban site).
Mean chemical composition (C) of the sub-micron aerosol ($\mu g/m^3$). Data represent similar conditions as for the N and V size distributions, but for case (a), (b) and (f) they are not obtained concurrently. The unknown fraction (unk) was calculated by comparing the sum of the quantified aerosol components with the sub-micron aerosol mass calculated from sub-micron particle volume size distributions (data not available at the urban and rural sites).

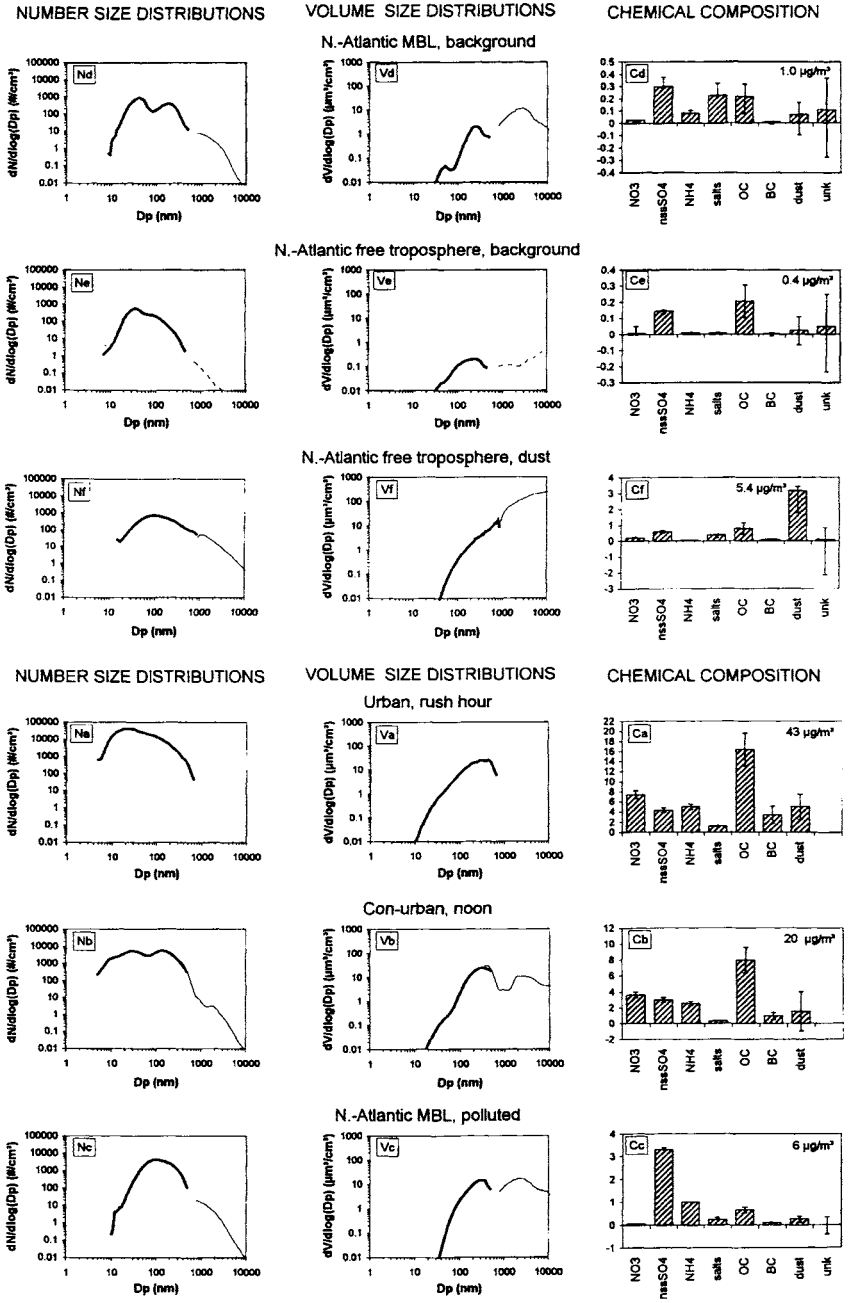
NUMBER SIZE DISTRIBUTIONS
VOLUME SIZE DISTRIBUTIONS
CHEMICAL COMPOSITION
N.-Atlantic MBL, background
N.-Atlantic free troposphere, background
N.-Atlantic free troposphere, dust
Urban, rush hour
Con-urban, noon
N.-Atlantic MBL, polluted
Nd
Vd
Cd
1.0 µg/m³
Ne
Ve
Ce
0.4 µg/m³
Nf
Vf
Cf
5.4 µg/m³
Na
Va
Ca
43 µg/m³
Nb
Vb
Cb
20 µg/m³
Nc
Vc
Cc
6 µg/m³
dN/dlog(Dp) (#/cm³)
dV/dlog(Dp) (µm³/cm³)
Dp (nm)
NO3
nssSO4
NH4
salts
OC
BC
dust
unk

from the aerosol precursor sources, condensation becomes too slow to maintain the continental aerosol loading, so aerosol volume decays.

2.2. Recent advances and remaining issues

Fig. 1 integrates knowledge that is available, at least qualitatively, since the middle of the 1980s. This knowledge resulted from theoretical developments (e.g. Fuchs, 1964; Friedlander, 1977) as well as key observations (Whitby, 1978; Hoppel et al., 1990; Section 3). However, during the last decade major progress has been made in dealing with the various chemical species that can be involved in one or more of the processes depicted in Fig. 1, and with the multicomponent nature of the atmospheric aerosol in general.

2.2.1. Nucleation

With respect to nucleation, it has in general been presumed that the principal gas-phase species involved in atmospheric nucleation is H_2SO_4, and that, if particle formation occurs, it does so via binary nucleation of H_2SO_4–H_2O (Jaecker-Voirol and Mirabel, 1989; Kulmala et al., 1998). Except for the case of cloud outflow (see below), observed rates of new particle formation significantly exceed predictions based on classical H_2SO_4–H_2O nucleation theory (Clarke et al., 1998a; Weber et al., 1996). It has been suggested that NH_3, an ubiquitous molecule in the troposphere, enhances nucleation rates of H_2SO_4–H_2O beyond the binary rate (Coffman and Hegg, 1995). Korhonen et al. (1999) have derived a ternary H_2SO_4–H_2O–NH_3 nucleation theory that predicts indeed substantial enhancement, and model studies predict an ubiquitous presence of stable H_2SO_4–H_2O–NH_3 clusters, which, however, remain too small to be detected ($D_p < 3$ nm) (Kulmala et al., 2000). Laboratory studies show that oxidation of volatile organic carbon (VOC) leads to new particle formation through nucleation. In the case of biogenic VOCs some oxidation products with low equilibrium vapour pressure have been identified (Christoffersen et al., 1998; Yu et al., 1999; Glasius et al., 1999). Regardless of the species involved, or the specific theoretical expression used for predicting nucleation, nucleation is a process that strongly depends on the gaseous precursor concentration, relative humidity and temperature. This implies that fluctuations in atmospheric conditions may play a major role in determining the location and magnitude of nucleation in the atmosphere (Easter and Peters, 1994). Such fluctuations might occur preferentially when mixing different air masses (Hegg et al., 1992; Nilsson and Kulmala, 1998). Finally it has been pointed out that nucleation around ions is energetically more favourable than homogeneous nucleation and that in certain atmospheric conditions it would dominate the particle formation process (Hamill et al., 1982; Raes et al., 1986). Recent theoretical developments including a whole range of ion–molecule and ion–ion

interactions, promote "ion-mediated nucleation" as the explanation to close gap between theory and observations (Turco et al., 1998).

At present, however, whether or not NH_3 or organics or fluctuations or ions are responsible for enhanced nucleation has yet to be verified experimentally.

2.2.2. Condensation

Semi-volatile species, like ammonium nitrate and many organics, will tend to distribute themselves between gas and aerosol phases to achieve thermodynamic equilibrium (Wexler and Seinfeld, 1990). Condensation occurs when the equilibrium shifts towards the aerosol phase.

In the case of inorganic species, the time scale over which this equilibration takes place has been analysed (Meng and Seinfeld, 1996); depending on the particle size and ambient conditions, equilibration times can vary from seconds to hours. Inorganic thermodynamic equilibrium models have been developed over the past two decades, reaching a state of maturity in terms of thermodynamic properties, such as condensed phase activity coefficient parameterizations, and computational implementation (Zhang et al., 2000). Originally developed to simulate gas–aerosol equilibrium in urban and regional-scale atmospheric models, inorganic gas–aerosol equilibrium models have now been embedded into general circulation models to predict the global distribution of sulphate–nitrate–ammonium aerosols (Adams et al., 1999). Predictions of the phase distribution of inorganic aerosol species are in general agreement with observations (Adams et al., 1999).

In the case of organic semi-volatile species much progress still is to be made. Because of the large number of such compounds in the atmosphere and because methods to predict their thermodynamic properties in complex organic-water mixtures pose significant theoretical challenges, gas–aerosol thermodynamic models for organic atmospheric species are not yet available. Experimentally based gas–particle distribution factors for complex mixtures generated by the photo-oxidation of hydrocarbons are available (Odum et al., 1996; Griffin et al., 1999b); however, the goal is fundamentally based thermodynamic models that predict the phase partitioning of individual organic compounds between the gas phase and complex organic–inorganic–water mixtures. Such models would allow first-principles prediction of the amount of organic aerosol formed from primary or secondary organic species in the atmosphere. Such models are currently under development.

2.2.3. Degree of chemical mixing

In treating multicomponent aerosols, the issue arises whether the components are mixed within a single particle (internal mixing), or whether the various components are present as pure particles (external mixing). The manner in

which different aerosol species are mixed in individual particles affects both optical and hygroscopic properties (Heintzenberg and Covert, 1990). The only processes depicted in Fig. 1 that lead to aerosols that are externally mixed from pre-existing aerosol are nucleation and primary emissions. The remainder of the processes lead to internal aerosol mixtures. The degree of "internal mixing", that is the degree to which the chemical composition of each individual particles resembles that of the bulk, will increase with the time available for interaction, hence with the residence time of the aerosol in the atmosphere. In urban and polluted continental conditions, the characteristic times of many of these interactions (see Table 2) are small, and internal mixing will occur on a short time scale. However, these regions provide generally also sources for primary and nucleated secondary aerosol, enhancing external mixing. Field observations have indeed shown that in continental areas, two distinct aerosol types with different hygroscopic properties are often present, a direct indication of externally mixed aerosol (e.g. Zhang et al., 1993; Svenningsson et al., 1994). In aged polluted air masses, such as found in continental plumes over the ocean, this feature is not observed, suggesting a chemically more homogeneous (sub-micron) aerosol (Swietlicki et al., 2000), in agreement with the long residence, hence interaction, times.

2.2.4. Aerosol activation

The understanding of activation of aerosols to cloud droplets, and, in particular, the role of organic species in this process, is rapidly evolving. Whereas before only the inorganic salts were considered to constitute the soluble aerosol fraction, it is now clear that a large fraction of aerosol organics is water soluble (Saxena et al., 1995; Saxena and Hildemann, 1996), and there is indirect evidence that these species contribute to the chemical composition of CCN (Novakov and Penner, 1993). Laboratory studies have shown that oxidation products of biogenic compounds, like terpenes, are only slightly hygroscopic; however, internally mixed with ammonium sulphate particles, these organic products do not inhibit water uptake by forming an impermeable layer, but rather mix homogeneously with the ammonium sulphate in the solution droplet (Virkkula et al., 1999).

The formation of layers is expected when organic surfactants are mixed with solution droplets. Surfactants have been found in fog droplets in polluted air masses, however their overall effect on the aerosol activation process is complex (Li et al., 1998). On the one hand, surfactants will reduce the surface tension of the droplets (as recently observed by Facchini et al. (1999)), hence decrease the supersaturation needed to activate them. On the other hand their presence will reduce the molality of the solution because of their high mole-

cular weight, and therefore increase the supersaturation needed to activate the droplet.

One further effect on aerosol activation is that, apart from water vapour, other soluble vapours can co-condense during the activation process, increase the solute content of the droplet and eventually decrease the supersaturation needed for activation. Theoretical work showed that in aerosol mixtures consisting of weakly soluble substances interacting with water vapour and other soluble gases present in the atmosphere (like HNO_3), particles can grow to cloud droplet sizes ($\sim$10 μm) at RHs below 100% (Kulmala et al., 1997). In order to describe the effects mentioned above, the traditional Köhler theory has been generalised to a multi-component multi-phase theory (Shulman et al., 1996; Kulmala et al., 1997).

All these studies indicate that the number of cloud droplets critically depends on the detailed physico-chemical properties of the initial individual aerosol particles, which in turn are determined by the complex of processes shown in Fig. 1.

3. Observations

3.1. Size distributions

Measurements of the atmospheric aerosol size distributions were essential in identifying the various processes involved in the formation and evolution of the atmospheric aerosol (Whitby, 1978; Hoppel et al., 1986, 1990). Jaenicke (1988) has reviewed such measurements up till the early 1980s and made a climatology of aerosol size distributions. Fig. 2 shows a similar climatology of number distributions and corresponding volume distributions as a function of particle diameter, obtained more recently by our groups with state-of-the-art aerosol counting and sizing equipment (Van Dingenen et al., 1995, 1999; Raes et al., 1997). They will be discussed in detail below. The improvement in aerosol measuring equipment is likely to be the main reason for the difference between the Jaenicke climatology and the present collection of distributions. Note that Fig. 2 shows the *dry* aerosol size, and that under ambient conditions the uptake of water may lead to a diameter growth by a factor up to 1.7. Log-normal parameters for the distributions in the sub-micron aerosol fraction (i.e. below 1 μm dry diameter) are given in Table 2.

3.1.1. Urban environment (traffic rush hour) (Fig. 2a)

The size distribution contains three modes. The maximum in the nucleation mode is around 15 nm diameter. This small particle mode appears consis-

tently during traffic rush hours in the morning and the evening, and can thus be linked to emissions from cars. The total particle concentration is of the order 3×10^4 cm^{-3}. Aitken and accumulation mode are merged into a broad mode. Considering the process time scales (Section 2), the Aitken mode can be explained by coagulation and condensational growth of nucleation mode particles, whereas the accumulation mode is a more aged aerosol, advected with the regional scale circulation, and formed by cloud processing and condensation.

3.1.2. Sub-urban environment (Fig. 2b)

The distribution shown is typical for a sunny summer day at noon. Also in this case numerous small particles are often observed, in particular when the total aerosol surface area is low. This indicates that these particles result from photochemically induced nucleation. Total number concentration is of the order $0.5–10 \times 10^4$ cm^{-3}. The high Aitken mode concentration is unstable with respect to coagulation (Table 2), indicating that it is freshly formed by coagulation and growth of the nucleation mode. The third mode is again the stable accumulation mode, aged (by cloud processing and coagulation) and advected into the area. A distinct coarse mode is also observed in the number and, a fortiori, in the volume size distributions. Chemical analysis shows that this mode contains mainly dust.

3.1.3. Polluted marine boundary layer (Fig. 2c)

The distribution represents a continentally derived aerosol which has advected for two days over the ocean. A fairly unimodal size distribution is observed below 1 μm, and a coarse sea-salt mode appears above 1 μm. The ultrafine particles observed in the continental aerosol have vanished, and number concentrations are reduced to about 2500 cm^{-3}. The time scales discussed above show that this type of distribution might further evolve through cloud processing. Although the size distribution still clearly shows a pollution signature (elevated number and volume compared to marine background), the two days of ageing in the MBL have made it chemically internally mixed, as shown by hygroscopicity measurements (Swietlicki et al., 2000).

3.1.4. Clean MBL (Fig. 2d)

The size distribution shows the typical tri-modal structure, with a pronounced Aitken mode, accumulation mode, and the coarse sea-salt mode. The minimum in particle number between the Aitken and accumulation mode is a result of cloud activation of those aerosols sufficiently large to act as CCN, followed by in-cloud chemical reactions and re-evaporation. In most cases no particles

smaller than 20 nm are observed, indicating that nucleation is not a major process in the remote MBL. The number is again reduced compared to the previous case and is in the range of 200–500 cm^{-3}.

3.1.5. Background lower free troposphere (2300 m asl) (Fig. 2e)

Size distributions generally have a multi-modal shape, with a dominant mode around 60 nm. Number concentrations range between 300 and 500 cm^{-3}. Recent observations (Maring et al., 2000) have shown that the mode round 60 nm correlated with Be-7, a tracer for upper troposphere air masses. Its form and number concentration have been explained by self-preserving theory (Lai et al., 1972; Raes, 1995), which, predicts that a coagulating and growing aerosol population eventually develops a (close to) lognormal size distribution and number concentrations that are independent of the initial size distribution and number concentration. The mode centred around 100–200 nm is related to anthropogenic tracers like sulphate (Maring et al., 2000). Background FT aerosol does not contain a significant coarse mode; the number of coarse particles is generally below 0.01 cm^{-3}.

3.1.6. Saharan dust layer (FT, 2300 m asl) (Fig. 2f)

This distribution illustrates a particular case of continentally derived aerosol (Saharan dust) injected into the FT and transported over long distances. The sub-micron aerosol shows a broad accumulation mode, in addition to a very pronounced coarse mode, obviously containing dust particles (some tens of coarse particles per cm^3 (Maring et al., 1999)). The accumulation mode is strongly enhanced compared to the 200 nm "pollution" mode in the background FT. The air masses into which the dust was injected, often contain anthropogenic pollution that was previously picked up. The interaction between these two aerosol types is of interest as it will determine the optical and cloud activation properties of the dust.

3.2. Chemical composition

Measurements of the chemical composition are important to identify the various sources contributing to the aerosol as well as its effect. Heintzenberg (1989) has reviewed the data until 1986 and reconstructed grand average chemical compositions for the sub-micron aerosol in a number of environments. Fig. 2 shows the average relative contributions of chemical compounds in the sub-micron fraction of the aerosols for the same environments discussed above. We will denote with PM1 the total aerosol mass in this size fraction.

3.2.1. Urban/sub-urban environment (Figs. 2a and b)

Preliminary chemical mass closure results indicate that the sub-micron urban aerosol is characterized by the highest PM1 concentration ($>40\ \mu g\,m^{-3}$), and the highest black carbon (BC) contribution (>8%). At a sub-urban site, 50 km away from a major urban centre, PM1 is already decreased by a factor of two. The aerosol sub-micron composition at the sub-urban site is close to what is observed at the urban site, except for primary aerosols, BC and dust which are significantly reduced. Organic compounds (OC) might represent the main component of the sub-micron aerosol a both urban and sub-urban sites (about 40%). However, OC data are affected by large and difficult to assess uncertainties (Putaud et al., 2000). At both sites, NO_3^- and SO_4^{2-} are fully neutralized by NH_4^+.

3.2.2. Clean and polluted MBL (Figs. 2c and d)

Chemical mass closure was achieved by comparing results of chemical analyses with size distribution measurements. The striking feature of the polluted MBL aerosol composition is the predominance of nss-SO_4. The polluted MBL nss-SO_4 concentration is indeed comparable to the rural site nss-SO_4 concentration. This could be due to the presence of specially important SO_2 sources (coal power plants?) upwind of the MBL sampling site, which was on Tenerife, Canary Islands. It is also interesting to notice that the contribution of NO_3^- to PM1 is very small. This can be explained by the displacement of the equilibrium $NH_4NO_3 \rightleftharpoons NH_3 + HNO_3$ above the ocean through the reaction of HNO_3 with sea salt:

$$NaCl + HNO_3 \rightarrow NaNO_3 + HCl.$$

Actually, the concentration of NO_3^- in the supermicron fraction averages $1.6\ \mu g\,m^{-3}$ in the polluted MBL, i.e. 20 times more than in the fine fraction. In the background North Atlantic MBL, nss-SO_4 remains the main PM1 component. Measurements of MSA, an indicator for DMS particulate oxidation products, suggest that oceanic biogenic sources could account for up to 50% of the background nss-SO_4. The relative contribution of OC is twice as high as in the polluted MBL. Even at moderate wind speed ($5\ m\,s^{-1}$), sea-spray contributes significantly to sub-micron aerosol mass in the background MBL (24%).

3.2.3. Background free troposphere (2300 m asl) (Fig. 2e)

PM1 is as low as $0.4\ \mu g\,m^{-3}$. OC may be the main component of the sub-micron aerosol. Estimation of the uncertainties in OC mean concentration in-

dicates that its contribution to the aerosol sub-micron mass is in the range 31–56%.

3.2.4. Saharan dust layer (FT, 2300 m asl) (Fig. 2f)

During transport events out of North Africa, mineral dust is the main component of sub-micron aerosol in the FT. However, the SO_4^{2-}/Ca^{2+} ratio observed during dust events is significantly higher than in fine Saharan sand grains and glacier ice cores representative of pre-industrial times (Schwikowski et al., 1995). This suggests that the desert dust plumes transported over the Atlantic Ocean tend to be mixed with pollution aerosol.

4. Modelling the clean marine boundary layer

The existence of significantly different size distributions and chemical compositions in various environments (see Section 3) has led the aerosol community to think in terms of atmospheric compartments, such as the marine boundary layer, the continental boundary layer, the free troposphere. Of those, the MBL has been studied extensively, because of its dominant role in the climate system (Charlson et al., 1987) and because of it simplicity relative to others.

The aerosol in the marine boundary layer (MBL) has traditionally been divided into two categories, that derived from sea salt and that from all non-sea salt (nss) sources. The dominant chemical component of the non-sea salt aerosol is sulphate. It has been established that the principal source of this sulphate in areas uninfluenced by anthropogenic sources, is gaseous DMS produced by phytoplankton in surface (Charlson et al., 1987; Ayers et al., 1991; Calhoun et al., 1991). A major question concerns the sensitivity of the levels of MBL aerosol number concentration to the sea-surface DMS emission rate, and correspondingly, the importance of other processes in controlling the levels of particles over the remote ocean (Bates et al., 1998).

The first studies dealing with this question, relied on box models of the MBL, and implemented descriptions of those processes in Fig. 1 dealing with sea-salt and sulphate aerosol formation (Raes and Van Dingenen, 1992; Russell et al., 1994). Model results, however, converged and were in better agreement with the observed size distributions only when entrainment of aerosol from the free troposphere was considered as a source of aerosol number in the MBL (Raes, 1995; Capaldo et al., 1999).

Indeed, whereas a few measurements have been reported of the occurrence of large numbers of ultrafine particles following rain events or strong subsidence of free tropospheric air (Covert et al., 1992, 1996; Hoppel et al., 1994b; Clarke et al., 1998a), observations generally indicate that subsidence from the

free troposphere is the main process controlling MBL aerosol number concentration (Clarke et al., 1996b; Bates et al., 1998; Raes et al., 1997; Van Dingenen et al., 1999, 2000).

In a recent study, Katoshevski et al. (1999) have simulated the relative influence of sources and sinks of particles using a simplified model of the clean MBL. Based on the typical conditions considered, MBL aerosol number concentration is predicted to be dominated by free tropospheric aerosol under virtually all conditions: 89% in the average case they consider, and even 69% at a 17 $m\,s^{-1}$ wind speed. MBL aerosol mass, on the other hand, is dominated by sea salt particles: 62% in the base case and 98% at a wind speed of 17 $m\,s^{-1}$. Even under conditions when a high rate of nucleation is presumed to occur, still only about 5% of the total particle number, on average, is predicted to be provided by nucleation events. Cloud processing, while not a major contributor to aerosol number, does provide, except under high wind conditions, the order of 20% of the aerosol mass. Although nucleation occurs only infrequently in the MBL and does not contribute appreciably to long-term average aerosol number or mass, nucleation can replenish particles in brief, intense episodes when aerosol surface areas are substantially reduced by precipitation.

In summary, the studies of aerosol formation and evolution in the clean MBL have highlighted that the aerosol characteristics observed within a certain compartment, cannot always be explained by processes occurring within that compartment. Instead, exchanges between compartments can play a major role. This is in agreement with the result of the time scale analysis in Section 2.1. We argue that it is necessary to consider general atmospheric circulation which connects marine and continental boundary layers and the boundary layer with the free troposphere, in order to understand the different characteristics of the aerosol throughout the global troposphere.

5. Global atmospheric circulation and the life cycle of the tropospheric aerosol

5.1. Tropospheric general circulation

Tropospheric general circulation is characterised by rapid, localized upward motion due to convection (in the tropics) or slantwise ascent along frontal surfaces (in the mid-latitudes), which is compensated by relatively slow and large-scale subsidence in the sub-tropical and polar regions. Horizontal transport in the lower and upper troposphere connects areas of upward and downward transport, in what are supposed to be toroidal circulation patterns. Long-term averages of both the meridional and zonal wind fields in the tropics/sub-tropics reveal the existence of these patterns, which are called the Walker and Hadley circulations, respectively (see Fig. 3). In a snapshot of the global wind fields,

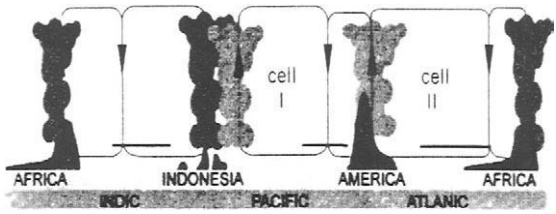

Figure 3. Global circulation in the tropics/subtropics, after Newell (1979). Convection occurs preferentially over the continents, whereas subsidence occurs over the oceans. The subsidence inversion creates a well-defined marine boundary layer, which is topped by stratiform clouds.

these toroidal circulations are less evident (Newell et al., 1996; Wang et al., 1998).

Subsidence over the sub-tropical oceans leads to the existence of a temperature inversion and the creation of a marine boundary layer, which is topped by vast stratiform clouds. Thus in the subtropics there is a clear separation between the marine boundary layer and the free troposphere aloft, whereas in convective regions this separation is less clear.

The general circulation is described by global observations of fields of winds and other meteorological parameters (Oort, 1983), or it can be reproduced by General Circulation Models (GCM's) from basic physical principles. Using the observed climatologies, or off-line versions of the GCMs, Chemical Transport models (CTMs) have been built in which the descriptions of emissions, transport, transformations and removal of chemical species have also been considered (Zimmermann, 1984; Heimann et al., 1990).

5.2. Recent progress and remaining issues

5.2.1. Global budgets and mass concentration fields of individual aerosol species

Major progress has been achieved in simulating the global distribution of tropospheric aerosol mass using global CTMs. The first simulation of the global distribution of biogenic and anthropogenic sulphur (Langner and Rodhe, 1991) lead to the recognition that anthropogenic sulphate aerosols may have a significant impact on the global radiation balance (Charlson et al., 1991). This spurred a large interest, and simulations of the global mass distributions for the aerosols types listed in Table 1 followed. Despite the simplification of considering each aerosol type independently, these studies were important to relate emissions to global distributions, to construct global and regional budgets, to estimate the contribution of anthropogenic sources to the burden of aerosol species that are also produced naturally, and to draw attention to elements of

the general circulation that are important in aerosol transport, in particular deep convection (Feichter and Crutzen, 1990).

5.2.2. The role of deep convection

The high updraft velocities in convective clouds and the corresponding supersaturations up to 2% lead to activation of soluble aerosol particles with diameters as small as 0.01 μm; partly soluble particles activate at somewhat larger diameters. Soluble trace gases in these updrafts will be taken up by the cloud droplets. Precipitation, which, on a global scale, is produced mainly in convective clouds, eventually removes the activated particles and dissolved gases. During convective cloud transport a separation therefore occurs between soluble species that are rained out and insoluble species that are pumped into the free troposphere (Rodhe, 1983).

Initially it was supposed that convective transport of fairly insoluble DMS and its subsequent oxidation to SO_2 and H_2SO_4 and MSA was the main source of sulphate aerosol in the background free troposphere (Chatfield and Crutzen, 1984). Recent simulations of convective transport (Wang et al., 1995) and, in particular, measurements over the Western Pacific (Thornton et al., 1997), now suggest that DMS contributes only 1–10% to the SO_2 in the upper troposphere over the Northern Hemisphere.

Fig. 4 shows the fraction of total SO_2 derived from DMS oxidation in the upper troposphere (300 mb) as simulated by the GISS GCM II' aerosol model (Adams et al., 1999; Koch et al., 1999). The simulation shown here is based on emissions from the IPCC SRES A2 scenario for the year 2000. This scenario prescribes 26.0 Tg S yr^{-1} of natural DMS emissions and 73.8 Tg S yr^{-1} of SO_2 emissions. Of the SO_2 emissions, 69.0 Tg S yr^{-1} stem from anthropogenic activities. The remaining 4.8 Tg S yr^{-1} represent volcanic emissions.

These results show that, in the northern hemisphere, SO_2 in the upper troposphere is mostly anthropogenic in origin. North of about 15°N latitude, less than 20% of the SO_2 is the product of DMS oxidation. In the most anthropogenically perturbed areas above the industrial centres of North America, Europe, and eastern Asia, the fraction is less than 10%, in agreement with the observations of Thornton et al. (1997) and results of Wang et al. (1995). The situation is mostly reversed in the southern hemisphere, where the SO_2 in the upper troposphere above remote ocean regions, such as the south Pacific and Indian oceans, is mostly derived from DMS oxidation. An important exception is a plume of anthropogenic SO_2 emissions visible above South America and Africa stemming from biomass burning and copper smelting activities in those areas.

Therefore, through the process of deep convection, anthropogenic activities have significantly perturbed not only the continental boundary layer, but also

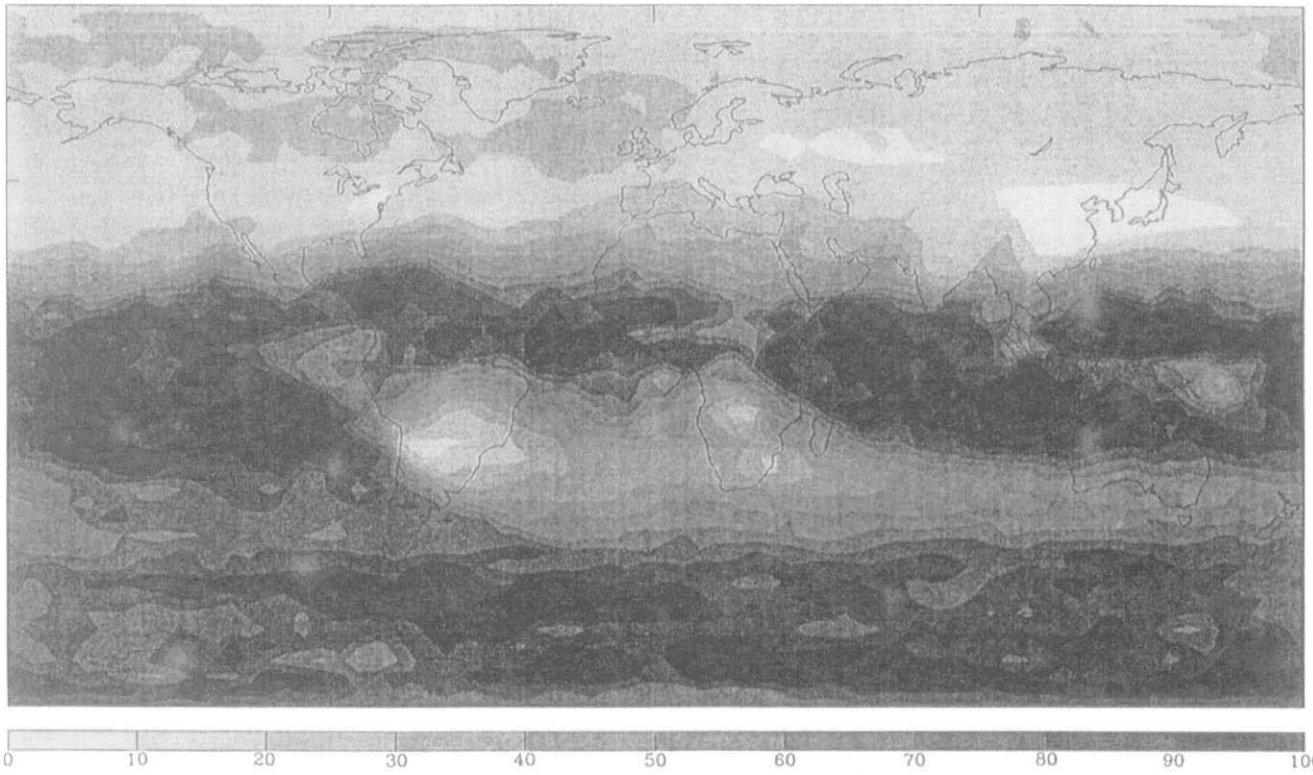

Figure 4. Fraction of total SO_2 derived from DMS oxidation in the upper troposphere (300 mb) as simulated by the GISS GCM II' aerosol model (Adams et al., 1999; Koch et al., 1999). Sulphur emissions were prescribed based on the IPCC SRES A2 scenario, including 26.0 Tg S yr^{-1} of DMS emissions, 69.0 Tg S yr^{-1} of anthropogenic SO_2 emissions, and 4.8 Tg S yr^{-1} of volcanic SO_2 emissions.

the free and upper troposphere as well. Because oxidation of SO_2 in the upper troposphere proceeds mainly by gas-phase reaction with the OH radical, anthropogenic activities have the tendency to increase gas-phase concentrations of H_2SO_4 in the upper troposphere. Given the low aerosol surface area concentrations in this part of the atmosphere, this process may result in enhanced rates of new particle formation in the upper troposphere.

5.2.3. Aerosol nucleation in the free troposphere

Deep convection leads to an increase of the photo-oxidizing capacity of the upper troposphere by pumping up nitrogen oxides produced by anthropogenic sources or biomass burning at the surface or by lightning within the convective cloud (Lelieveld and Crutzen, 1994; Jacob et al., 1996). Given the link between photochemistry and aerosol formation (see Fig. 1), as well as the increase in gas-phase concentrations of H_2SO_4 discussed in the previous section, a link between convective clouds and aerosol nucleation might be expected.

Measurements in the upper troposphere of the Pacific demonstrate an anti-correlation between aerosol number and aerosol surface area (Clarke, 1992, 1993; Andronache et al., 1997), suggesting that production of new particles by nucleation occurs when the pre-existing aerosol surface area is low, in agreement with the process understanding. These measurements show, furthermore, enhanced ultrafine particle concentrations above the convective areas of the Inter Tropical Convergence Zone. Other data indicate that conditions favourable for nucleation exist near evaporating cloud boundaries in both mid-latitude and equatorial marine environments, i.e. elevated water vapour, cold temperatures, low aerosol surface areas (about 5 $\mu m^2\ cm^{-3}$) or a combination of these (Hegg et al., 1990; Perry and Hobbs, 1994; Clarke et al., 1998b). The high actinic flux in the vicinity of clouds can furthermore increase OH production (Mauldin et al., 1997), which, in turn, enhances formation of H_2SO_4 vapour. As noted in Section 2.3, observations that include measurements of gas-phase H_2SO_4 have detected nucleation events near clouds, in agreement with the predictions of the classical theory (Clarke et al., 1999). In this way, convective clouds seem to both initialize the life cycle of part of the background aerosol and terminate it, when, after going through the Hadley/Walker circulation, particles re-enter a convective cloud and are removed by precipitation.

Measurements at various sites in the remote troposphere indicate that the rate at which freshly formed particles grow exceeds that which can be explained by condensation of H_2SO_4 and associated H_2O (Weber et al., 1998; Kulmala et al., 2000). It has been suggested that condensation of other compounds (notably organics) on the nucleated H_2SO_4–H_2O–NH_3 clusters might account for this "excess" growth.

5.2.4. Organics aerosol in the free troposphere

Organic aerosol has been observed to be ubiquitous in the upper troposphere (Novakov et al., 1997; Murphy et al., 1998b; Putaud et al., 2000, Section 3.2). Although the accuracy of organic matter determination in aerosols is in question, these studies do claim that there is relatively more organic matter in the upper troposphere than sulphate. This would be consistent with a separation between soluble and insoluble species during vertical transport.

A major question is the extent to which organic aerosol in the upper troposphere is derived from atmospheric oxidation of biogenic hydrocarbons to organic aerosol products. Such organic aerosol can reach the free troposphere by two routes. Deep convection over tropical areas could transport relatively insoluble biogenic hydrocarbons into the free troposphere where they are oxidized to produce organic aerosol or oxidation and aerosol formation can occur in the boundary layer, with the aerosol subsequently being transported to the free troposphere.

Biogenic hydrocarbons such are terpenes are among the most reactive gaseous compounds in the atmosphere, and they are important precursors of secondary organic aerosol (Went, 1960; Christoffersen et al., 1998; Griffin et al., 1999a; Glasius et al., 2000). Terpene oxidation occurs by reaction with OH, O_3, and NO_3, with OH and O_3 being generally the most important under atmospheric conditions. Laboratory chamber data on the aerosol-forming potential of individual terpenes, together with temporally and spatially resolved, compound-specific estimates of global biogenic hydrocarbon emissions and global OH and O_3 fields, can be combined to obtain an estimate of the annual global production of organic aerosol from biogenic hydrocarbons. This procedure has been employed to lead to an estimate of 18.5 Tg per year of present day biogenic organic aerosol production (Griffin et al., 1999b). Because of the high reactivity of the biogenic parent compounds with OH and O_3, most of the oxidation is predicted to occur in the lowest few kilometers of the atmosphere. One aspect of the process that the estimate of Griffin et al. (1999b) does not account for is the effect of temperature on the conversion of oxidation products to aerosol. As temperature decreases, semi-volatile oxidation products will increasingly partition to the aerosol phase; thus, all else being equal, the above estimate can be considered to be conservative, since it is based on aerosol yields measured at room temperature.

With an assumed free troposphere residence time of two weeks, this annual global formation rate leads to an estimate of the average mass concentration of tropospheric organic aerosol derived from biogenic hydrocarbons of about 0.5 $\mu g\, m^{-3}$. Such an estimate has necessarily a considerable degree of uncertainty associated with it, easily plus or minus a factor or two. The estimate does not account for, for example, the effect of wet scavenging of terpene ox-

idation products in deep convection, although such products are not expected to be overly hygroscopic (Virkkula et al., 1999). Nevertheless, the estimate 0.5 $\mu g\, m^{-3}$ can be compared with the 0.4 $\mu g\, m^{-3}$ measured in the North Atlantic free troposphere (Putaud et al., 2000, Section 3.2), and does suggest that terpene oxidation is a potential contributor to organic aerosol in the free troposphere and that the route of injection by convective mixing of boundary layer oxidation products can lead to measurable levels of such aerosol.

5.2.5. Ubiquity of layers in the troposphere

Recent observations have shown that the free troposphere is chemically not homogeneous. Quasi-horizontal layers are frequently observed which are characterised by various combinations of ozone and water vapour (Newell et al., 1999), and other chemical species (Wu et al., 1997). Layers with lower O_3 and higher H_2O than the background are tentatively interpreted as due to convection from the boundary layer. Layers with higher O_3 and lower H_2O, which are the most abundant are interpreted as originating in the stratosphere. Vertical profiles of aerosols also indicate layered structures in, e.g. aerosol number concentration (e.g. Clarke et al., 1996) but a detailed study of their relationship with other gas-phase species has not been made yet. Convective transport of (insoluble) pollution aerosols or nucleation near clouds might be two ways of producing such layers in the middle and upper troposphere. Johnson et al. (2000), however, observed layers in the lower free troposphere immediately above the marine boundary layer, which they explained as originating from a deep (2–5 km) convectively driven continental aerosol layer which advects over the colder ocean. Layers of mineral dust from the Gobi and Sahara desert are frequently found over the Pacific and Atlantic oceans, respectively.

Turbulent mixing in the free troposphere is extremely slow. Following the formulation of Dürbeck and Gerz (1996), the time needed to mix a layer throughout the depth of the free troposphere is larger than the time needed to subside a layer from the upper free troposphere to the surface, the latter being about 10–14 d (Gage et al., 1991). Hence, interaction and mixing of aerosols in different free tropospheric layers, might not happen often. Evidence for this lack of mixing is given by Ostrom and Noone (2000), who measured different aerosol properties at different heights within the same Saharan dust outbreak over the N. Atlantic.

6. Aerosol microphysics in the context of the general circulation

A straightforward way to link microphysics and the general circulation and treat fully the issues discussed above is to implement the descriptions of the

processes depicted in Fig. 1 in a general circulation model or global CTM, which captures the transport patterns depicted in Fig. 3. However, in order to accurately treat aerosol dynamic processes such as nucleation, coagulation, and condensation, the aerosol size distribution between 1 nm and 1 μm should be described with a high resolution in particle size (Raes and Van Dingenen, 1995). Furthermore, within each size class several chemical compounds should in principle be tracked. Hence, the model must handle a large number of extra tracers, which is computationally not possible yet. Simplified descriptions of the multi-dimensional size distributions are still in order. Another problem with GCMs or global CTMs is their low spatial resolution (presently 100 × 100 km at best). The discussion in the previous sections identified various processes that are likely to be important at a smaller scale; this is particularly the case with cloud processes, nucleation, and with the existence of fine horizontal layers in the vertical. Parameterization of these sub-grid processes are also needed: they might be developed with box models which are more appropriate to describe detailed microphysical processes in air parcels or layers and to probe how these processes are sensitive to elements of the global circulation.

In the following sections we give an example of both box and 3-D modelling approaches, including some initial results.

6.1. Diagnostic 0-D modelling of aerosol microphysics and global circulation

Raes et al. (1993) used a box model in which they implemented the aerosol dynamics processes of Fig. 1, related only to the H_2SO_4–SO_2 aerosol system as it results from biogenic DMS emissions over the oceans and excluding the primary emissions of seasalt. They "moved" this box through an oceanic Hadley/Walker cell (cell I in Fig. 3). This approach turned out to be adequate to study in a qualitative way the cycling of aerosols in the clean marine environment. It predicted, in particular, the occurrence of nucleation in the outflow regions of the convective clouds, and the absence of nucleation within the MBL.

This simulation is repeated here with an updated version of the aerosol dynamics model, AERO3, which considers also the primary emissions of insoluble soot particles (Vignati, 1999, see Appendix B). The inclusion of soot allows one to study also aerosol cycling in a Hadley/Walker cell that has its convective updraft over the polluted continent (cell II in Fig. 3).

In both the clean marine and polluted continental scenario the simulation starts with the aerosol that enters a convective cloud. In cloud, the fraction of SO_2 oxidised in the cloud droplets and the fraction of the aerosol that is activated at a supersaturation of 2% is completely removed by precipitation. DMS, the remainder of the SO_2 and the unactivated aerosol is injected into

the Free Troposphere (FT), where an immediate dilution by a factor of 4 is assumed to account for the turbulent mixing at the exit of the cloud. This factor is in agreement with the reduction of DMS measured below and near the top of convective clouds (Ferek et al., 1986). Subsequently the aerosol plume travels for 15 d in the FT, where it is slowly dispersed due to atmospheric turbulence (Dürbeck and Gerz, 1996). In the plume DMS is oxidized by OH to SO_2 and further to H_2SO_4. If the conditions allow, nucleation can occur, in which case the aerosol further develops by coagulation and condensation. As a rough simulation of the conditions expected in the free troposphere, the plume experiences 90% relative humidity during the first day after leaving the cloud. Afterwards the relative humidity is kept at 40%. During the first 8 d of the simulation, transport is kept at constant height in the FT and the temperature is maintained constant at 239 K. During the last 7 d the plume subsides, and the temperature increases linearly to the MBL value. After 15 d, the aerosol entrains into the MBL, where it travels for another 7 d back to its starting point. In the MBL the SO_2 concentration responds to the oxidation of locally emitted DMS with OH radicals, and the MBL aerosol size distribution is governed by the aerosol dynamical processes, by cycling trough MBL clouds and by entrainment of the free tropospheric aerosol. The free tropospheric aerosol is that resulting after the initial 15 d of transport in the FT. A comprehensive list of input data to the model is given in Table 3.

Table 3. Input data for the AERO3 diagnostic box model calculations, shown in Fig. 5[a]

	Free troposphere	Marine boundary layer
Temperature (K)	239	279
Relative humidity (%)	99 decreasing to 40	90
Background SO_2 (pptV)	20	
Initial SO_2 (pptV)		20 (CM) 840 (PC)
Initial DMS (pptV)		80
OH 24 h average (mol cm^{-3})	2×10^6	2×10^6
DMS flux (μmol m^{-2} d^{-1})		5
H_2O_2 (pptV)	500	500
pH of cloud	5	5
LWC (g m^{-3})	0.3	0.3
Supersaturatio (%)	2 (convective cloud)	0.2 (stratiform cloud)
Cloud cover (%)		43
Removal efficiency by precip (%)	100	15
Boundary layer height (m)		1500

[a]CM = Clean Marine Case; PC = Polluted Continental Case.

6.1.1. Clear marine case (Cell I)

The model is initialised with the bi-modal clean MBL aerosol size distribution in Fig. 2d and with log-normal parameters given in Table 2. (Note that this bi-modality is hardly resolved in Fig. 5a.) The particles are assumed to be pure H_2SO_4–H_2O droplets. Fig. 5 shows the evolution of the number size distribution. At time zero the total particle number sharply decreases, as all particles larger than a (dry) critical diameter of 20 nm are processed and eventually removed in the convective cloud. The surface of the aerosol (at 90% rh) is reduced from 32 $\mu m^2\ cm^{-3}$ in the MBL to 0.0175 $\mu m^2\ cm^{-3}$ when exiting the cloud. This small surface area, together with the initial high relative humidity and the low temperatures, leads to a burst of nucleation of new particles. After the first day the particle number steadily decreases due to coagulation, while condensation of H_2SO_4 increases the aerosol mass. The distribution after 15 d of transport in the FT is mono-modal, in agreement with measurements at the free tropospheric station of Izana only in the cleanest conditions (Raes et al., 1997). When after 15 d this aerosol entrains into the MBL, in-situ MBL nucleation is quenched by the surface area of the entrained aerosol, despite the increase in relative humidity and DMS derived H_2SO_4 in the gas phase. Entrainment and MBL cloud processing determine the final aerosol size distribution. The mode at $D_{p,dry} = 40$ nm is due to the shape of the FT size distribution, while the second mode is formed by the cloud processing in the MBL stratiform clouds. The fact that after going through one cycle the size distribution exhibits the same basic bi-modality as the initial size distribution supports the sequence of microphysical and dynamical processes used to explain these size distributions.

According to this model, formation by nucleation in the upper troposphere in cloud outflow and subsequent coagulation during subsidence would explain the observed increase in total number concentration with increasing altitude over the remote oceans (Clarke et al., 1993, 1998; Andronache et al., 1997). Condensation increases the aerosol mass and shifts the aerosol size distribution towards larger sizes, but due to the decreasing availability of SO_2 the importance of the process diminishes during transport in the FT. Entrainment of free tropospheric particles in the MBL is the process determining the final MBL particle number, whereas cloud processing by marine stratus clouds is the main contributor of the aerosol mass increase. This is in agreement with the discussion in Section 4.

6.1.2. Polluted continental case (Cell II)

The difference with the previous simulation is that the model is initialised with an aerosol size distribution and SO_2 concentration, typical of continen-

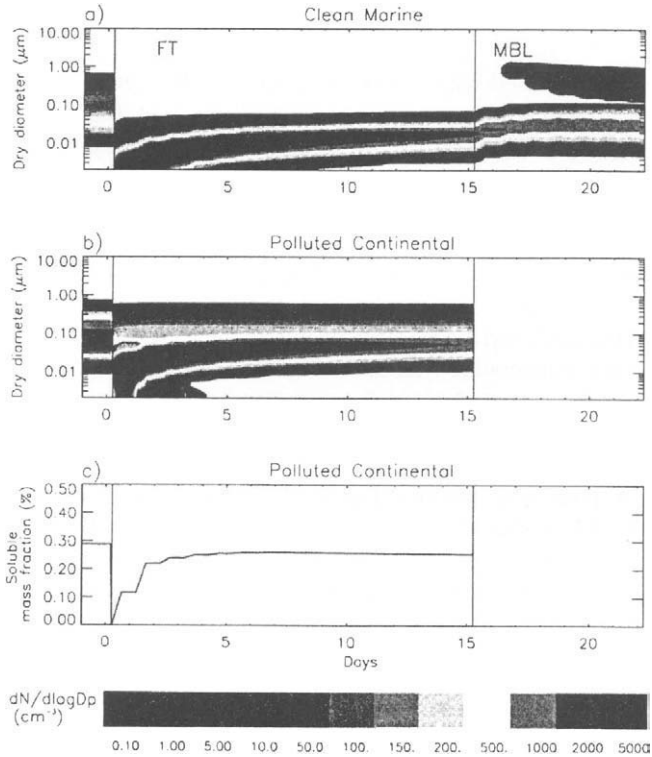

Figure 5. (a) Modelled time evolution of the number size distribution of H_2SO_4–H_2O particles in an air parcel cycling through a clean marine circulation cell (Cell I in Fig. 3). At $t = 0$, the parcel is transported through a convective cloud over the ocean. The concentration is initially reduced by activation and wet deposition. A burst of nucleation is predicted at the outflow of the cloud in the upper troposphere. The number decreases mainly by coagulation and the particles grow by coagulation and condensation during 15 d of transport in the FT. On day 15, the aerosol is entrained in the marine boundary layer to form the MBL Aitken mode. Nucleation within the MBL is quenched by the entrained aerosol surface area, but an accumulation mode develops through cloud processing. (b) Modelled time evolution of the number size distribution of internally and externally mixed Black Carbon–H_2SO_4–H_2O particles in an air parcel cycling through a polluted marine circulation cell (Cell II in Fig. 3). At $t = 0$, the parcel is transported through a convective cloud over the polluted continent. The concentration is initially reduced by activation and wet deposition. A burst of nucleation is predicted at the outflow of the cloud in the upper troposphere, despite the higher number of particles surviving wet deposition. The number decreases mainly by coagulation, and the particles grow by coagulation and condensation during 15 d of transport in the FT. After 15 d of evolution in the FT the aerosol is bi-modal (however not resolved in the figure) with the smallest particles consisting of pure H_2SO_4–H_2O particles and the larger of mixed BC–H_2SO_4–H_2O particles. The form of the distribution is comparable with the one shown in Fig. 2e. (c) Soluble mass fraction of the aerosol. At $t = 0$ the soluble mass fraction decreases as the most soluble aerosol is activated in the cloud and removed by precipitation. The soluble mass fraction subsequently increases by condensation of H_2SO_4.

Table 4. Characteristics of the input distributions for the AERO3 box model calculations shown in Fig. 5

		Clean marine	Polluted continental
Aitken mode (dry)	N (cm^3)	300	2800
	D_p (nm)	36	76
	σ	1.42	1.52
Accumulation mode (dry)	N (cm^3)	70	350
	D_p (nm)	150	230
	σ	1.47	1.36
Soluble fraction	ε (%)	100	28[a]

[a]Of the particles with diameter smaller than 0.3 μm 50% are assumed to be purely insoluble, and 50% internally mixed with ε equal to 0.52. Of the particles larger than 0.3 μm 20% are considered purely insoluble and 80% internally mixed with ε ranging between 0.52 and 0.90, to obtain an average ε equal to 0.28. Pure soluble particles are considered initially zero.

tal polluted conditions. The aerosol is an external/internal mixture consisting of water-soluble H_2SO_4 and insoluble soot. The average water-soluble mass fraction is 28%, and its distribution across the size distribution has been determined using results from various experiments looking at either the hygroscopicity (Svenningsson et al., 1994) or the solubility of the aerosol (Sprengard-Eichel et al., 1998) (see Table 4). Figs. 5b and c show the evolution of the number size distribution and soluble mass fraction of the aerosol, respectively. Only the insoluble and part of the mixed particles survive wet deposition in the convective cloud, and the aerosol surface is reduced from 144 $\mu m^2\,cm^{-3}$ in the boundary layer to 6.2 $\mu m^2\,cm^{-3}$ at the exit of the cloud. Although this offers a larger surface area for condensation than in the clean case, nucleation still does occur because of the larger concentration of SO_2 that survives through the cloud. Twelve hours after the injection in the FT, condensation of H_2SO_4 and coagulation with the nucleated soluble particles have transformed the remaining insoluble particles into mixed particles. During the FT transport the total number of new particles, which initially are mainly soluble, decreases due to coagulation, whereas the soluble mass fraction keeps increasing due to condensation. After 15 d of transport in the FT, the distribution is bimodal, with the largest mode being the boundary layer aerosol, modified by convective transport and transport in the FT, and the smallest mode the new aerosol nucleated near the convective cloud. The bimodal distribution is in qualitative agreement with most measurements at the free tropospheric site of Izana (see Fig. 2e), and the interpretation of these distributions by Maring et al. (2000) (see above) supports the sequence of events described by the model.

6.2. CTM 3-D modelling of aerosol microphysics and global circulation

A "modal" model, M^3, for H_2SO_4–H_2O aerosol dynamics has been developed, in which the aerosol size distribution is represented by overlapping log-normal size distributions representing, respectively, the nucleation mode, Aitken mode and accumulation mode (Wilson and Raes, 1996, see Appendix C). This model is used to resolve the particle size and number concentration of the sulphate mass calculated by a model of the atmospheric global sulphur cycle (Langner and Rodhe, 1991). It is further coupled to a model of the atmospheric black carbon (BC) cycle (Cooke and Wilson, 1996), and a static sea salt aerosol distribution (Blanchard and Woodcock, 1980), which together provide a background aerosol for the H_2SO_4–H_2O dynamics processes to interact with. This coupled model is implemented in the global off-line CTM TM2 (Heimann et al., 1990). Hence, in each gridbox of the CTM, the model treats the processes depicted in Fig. 1: the secondary aerosol consists of H_2SO_4–H_2O resulting from the oxidation of biogenic DMS and anthropogenic SO_2, or from in-cloud oxidation of SO_2, and the primary aerosol consist of sea salt and of black carbon from fossil fuel and biomass burning. Dust and organics are not included. Details on the global emission inventories for DMS, SO_2, H_2SO_4 and black carbon used are given in Appendix C, Table 5.

The model is run for 3 yr with meteorology and emissions representative of the mid–1980s, and the results discussed below pertain to the third year of the

Table 5. Input data for the M^3-TM3 CTM model calculations, shown in Fig. 6

Transport Model TM2	
Basic reference	Heimann et al. (1990)
Resolution	8° × 10° × 9 levels
Meteorology	ECMWF 1987
Clouds	ISCCP monthly mean cloud data
Photo chemistry	prescribed monthly average OH, O_3 and H_2O_2 from TM3 (Dentener, personal communication)
Global emissions and fields	
DMS	Bates et al. (1987)
SO_2	GEIA v1A 15% of SO_2 emitted as H_2SO_4 (70% attached to BC 30% as gas)
Black Carbon	Mass based emissions from Cooke and Wilson (1996) Transformed into number based emissions assuming a lognormal distribution with geometric mean diameter of 60 nm and a geometric standard deviation of 2.0
Sea salt	Mass loading after Blanchard and Woodcock (1980) Transformed into number concentrations assuming a lognormal distribution with geometric mean diameter of 600 nm and geometric standard deviation of 1.8

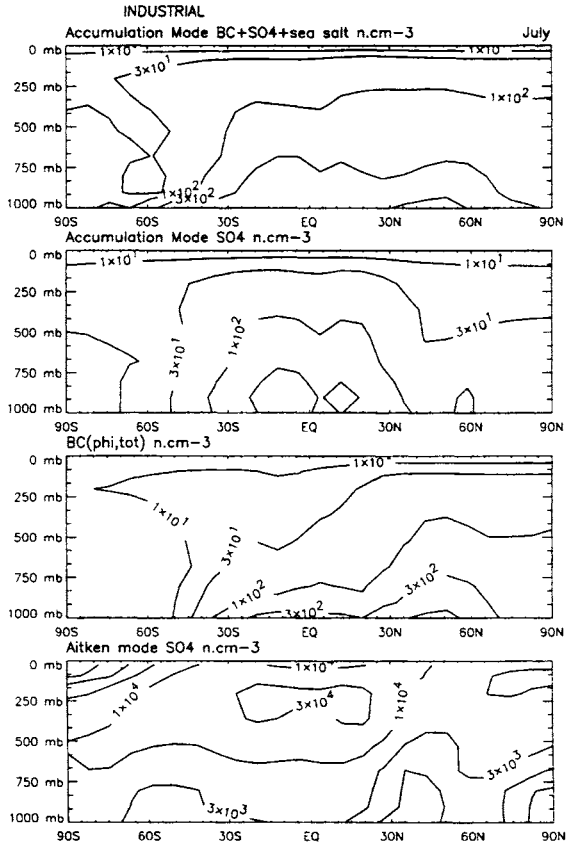

Figure 6. Zonal plots of aerosol number concentration as calculated with a global Chemical Transport Model (see text for full description): (a) total number of accumulation mode particles ($D_{p,dry} > 80$ nm) including pure BC, pure H_2SO_4–H_2O, mixed BC–H_2SO_4–H_2O particles and sea-salt particles; (b) number of pure H_2SO_4–H_2O accumulation mode particles; (c) number of internally mixed BC–H_2SO_4–H_2O accumulation mode particles; (d) number of pure H_2SO_4–H_2O particles in the Aitken mode ($10 < D_{p,dry} < 80$ nm).

simulation. Fig. 6 shows the resulting zonally averaged fields for July, of the number concentration in several aerosol classes.

Fig. 6a shows the concentration of the total number of accumulation mode particles ($0.08 < D_p$), including pure BC, pure H_2SO_4–H_2O particles, mixed BC–H_2SO_4–H_2O particles and sea-salt particles. In the clean Southern Hemisphere the number concentration is between 30 and 300 cm^{-3} at the surface. In the northern hemisphere, the zonally averaged number concentration increases to between 300 and 1000 cm^{-3} at the surface, as a result of the an-

thropogenic emissions. Accumulation mode number concentrations generally decrease with height.

Fig. 6b shows the number of pure H_2SO_4–H_2O accumulation mode particles. They are confined to the lower layers in the atmosphere, as they are removed by wet deposition in convective clouds, but are not affected by subcloud scavenging in the model.

Fig. 6c shows the mixed BC–H_2SO_4–H_2O accumulation mode particles. They typically comprise a larger fraction of the total than the pure H_2SO_4–H_2O accumulation mode particles. Because of the reduced solubilty of BC when emitted, the model transports them more effciently through convective clouds into the upper troposphere.

By differencing Fig. 6a with Figs. 6b and c, it can be seen that in the mid-lattitudes and polar regions the number of accumulation mode particles is governed by the primary emissions of sea salt.

Fig. 6d shows the pure H_2SO_4–H_2O particles in the Aitken mode ($10 < D_p < 80$ nm). In the model, these particles are only formed from the growth of nucleation mode particles. Their concentration is greatest in the upper troposphere, in particular in the outflow regions of the tropical convective clouds. A lesser maxima is found in the Northern Hemisphere at the surface, near the anthropogenic SO_2 source regions, and overall zonal average surface concentrations are in the range 300–3000 cm^{-3}. The same features are also seen in the nucleation mode concentration fields (not shown).

There is a lack of global aerosol size distribution data so that it is not possible to reconstruct decent zonal averages from measurements and test the model results presented above (Heintzenberg et al., 2000). However, a comparison with individual data sets is possible. The results of Fig. 6a, e.g., are in general agreement with the data on accumulation mode particles ($N_{D_p>80\,nm}$) shown at the bottom of Table 2. The measured urban and sub-urban aerosol number concentrations are 4500 and 2700 accumulation mode particles cm^{-3} respectively, but these high values pertain to local situations which most likely are smeared out in a zonal average of a CTM. Observations over the ocean, downwind of polluted continental areas indicate an internal mixture of the aerosol, with the number of the accumulation mode aerosol being governed by a refractery aerosol, most likely black carbon (Clarke et al., 1996b). The predominant role of sea salt in determining the number of accumulation mode particles in certain marine areas of high wind speed such as the mid-latitutes has been documented by Murphy et al. (1998a). The decrease in accumulation mode particles and increase in Aitken mode particles with altitude are in agreement with vertical profile measurements. However, the predicted zonal average Nucleation and Aitken mode concentrations are larger throughout the model domain than observations suggest. For example in the FT, the modelled zonal average concentrations (3000–30,000 cm^{-3}) have been observed only

locally near the outflow of clouds. We believe the over-prediction in Aitken mode concentrations is driven by nucleation in the free troposphere; consequently, the effect is seen most strongly in the FT and less so at the surface and in the accumulation mode zonal average concentrations. The two model layers spanning 70–255 mbar, have minimum temperatures of 190 and 210 K, respectively. At these temperatures and 30% RH, the modified formulation of Jaecker-Voirol and Mirabel used in M^3 effectively nucleates all gas phase sulphate concentrations in excess of 10^2 and 10^5 molecules cm^{-3}, respectively. While the nucleation parameterization is obviously playing a big role in the excess particle formation predicted in the FT, this does not preclude a contribution from the chemistry of the FT yielding too much OH oxidation of SO_2. This could be due to the simplified DMS chemistry scheme, or over abundant OH concentrations, or under-prediction of cloud volumes.

7. Summary and outlook

During the past decade enormous progress has been made in the understanding of the life cycle of aerosols in the global atmosphere. In the previous sections we argued that even a basic understanding of aerosols at a global scale requires the understanding and integration of both microphysical and large-scale dynamics processes. This is primarily because the time scales of aerosol evolution are in many cases longer than the residence time in particular atmospheric compartments. Furthermore, important phenomena such as nucleation and particle wet removal are occurring at the boundary of such compartments.

At present, however, the picture of the aerosol life cycle remains fragmentary. Observational data sets are incomplete and models need to take simple approaches, favouring one aspect of the aerosol (e.g. calculation of aerosol mass) at the expense of others (e.g. calculation of aerosol number). Based on the process understanding, observations and model calculations presented in this paper, the following general statements are tentatively made.

- In areas of strong primary emissions (e.g. sea salt over the ocean at high wind speed, black carbon in industrial areas) secondary aerosol species will preferentially condense on the primary particles, and the number of the resulting mixed particles will be determined by the latter. Even if nucleation does occur, the freshly nucleated particles are expected to coagulate with the primary aerosol within 1–2 d, and eventually the primary particles will again govern the number concentration of the aerosol.
- The removal of the aerosol in the 0.01–1 μm diameter range is mainly through activation in clouds and subsequent precipitation. The efficiency of this wet removal process depends on the size and chemical composition of the aerosol, which itself results from the complex of aerosol dynamic

processes. Although essential in determining the aerosol burden, wet removal is the least understood.

- Assuming a 100% wet removal of particles activated in convective clouds, conditions at the outflow of convective clouds are favourable for nucleation both when the convection occurs over the remote ocean and when it occurs over the polluted continent.
- The convective updraft of DMS over the remote ocean and SO_2 over the polluted continent is sufficient to induce nucleation of H_2SO_4–H_2O in the upper troposphere. Measurements and global budget calculations suggest however that half of the free tropospheric aerosol *mass* might be organic in nature.
- The number concentration of the FT aerosol is governed by the initial nucleation bursts and subsequent coagulation. These processes are expected to be happening in isolated layers originating at the convective cloud outflow.
- Entrainment of FT layers in the boundary layer might constitute a source of particle number, e.g. in case of the clean marine boundary layer, or it might dilute the BL aerosol when the latter is polluted.

In this paper a discussion on the effects of changing emissions or climate change on the global aerosol has not been attempted. A complex web of chemistry–aerosol–climate interactions exists, which makes any calculation of the future aerosol system speculative. The tropospheric aerosol system is nonlinearly dependent on the meteorological and chemical variables that govern its behaviour. Emissions of sea salt, mineral dust, and DMS increase nonlinearly with increasing wind speed. Hence, a future climate characterised by altered wind speeds would experience different amounts of natural aerosols. Nucleation rates depend nonlinearly on temperature, relative humidity, and vapour concentrations. Small changes in temperature and water content can produce large changes in new particle formation rates. However, coagulation serves to damp the effect of such excursions. Aerosols are the nuclei around which clouds form, and cloud properties depend in a nonlinear way on the quantity and composition of available particles. In a future atmosphere in which particle number concentrations are different in number and composition, e.g. by changing emission of primary particles and secondary precursors in industrial areas, cloud properties are likely to be changed. Such changes could result in altered cloud prevalence and convection that, in turn, would affect the aerosol life cycle through modified patterns of deep convection and wet removal. Increase of NO_x imported into background regions can affect the abundance of OH and thus the oxidising capacity of the troposphere, which could affect the rate of oxidation of SO_2 and organics to produce condensable species. Alteration of aerosol levels can affect tropospheric actinic flux and atmospheric photolysis rates that, in turn, change the rate of generation of OH itself.

The life cycle of the tropospheric aerosol is intimately interwoven with the climate–atmospheric chemistry system. To predict how the tropospheric aerosol will respond to climate change will require deep understanding of the dynamics of the climate system itself.

Appendix A

We use as the characteristic time the "e-folding time" τ, i.e., the inverse relative rate of change of a property (aerosol number, volume, diameter, etc.) through a process (coagulation, condensation, etc.). For instance, the characteristic time for change of number by dry deposition is given by

$$\tau_{N,\mathrm{dry}} = \frac{1}{N}\frac{\mathrm{d}N^{-1}}{\mathrm{d}t} = \frac{1}{\lambda_{\mathrm{dry}}},$$

by coagulation by

$$\tau_{N,\mathrm{coa}} = \frac{1}{N}\frac{\mathrm{d}N^{-1}}{\mathrm{d}t} = \frac{1}{KN}.$$

The characteristic times for coagulation given in Table 2 are those for depletion of aerosol number in the various modes by coagulation with Aitken and accumulation mode particles, and with cloud droplets. Coagulation rates are obtained from the coagulation coefficients for monodisperse particles of typical nucleation, Aitken and accumulation mode size with Aitken, accumulation and cloud droplet size particles, respectively (Seinfeld and Pandis, 1998). For the coagulation with cloud droplets the average time an air parcel spends in and outside clouds is taken into account (Lelieveld et al., 1989). Coagulation plays a significant role in the atmosphere when particle number concentrations are high and/or residence times are long. Small particles coagulating with larger ones do not significantly increase the mass of the larger particles, but the process reduces the number of small particles.

The characteristic time for the change in volume by condensational growth is derived assuming that the rate-limiting step is the oxidation of SO_2 in the gas phase. The amount of sulphate produced per unit of time is then distributed over the aerosol modes, weighted by the surface area in each mode and $\tau_{V_i,\mathrm{cond}}$ is obtained as (Van Dingenen et al., 2000)

$$\frac{1}{V_i}\frac{\Delta V_i^{-1}}{\Delta t}.$$

The contribution of aqueous-phase chemistry is estimated by transferring all available gas-phase SO_2 to accumulation mode-SO_4 during 20% of the time,

the latter being the average time an air parcel spends inside clouds (Lelieveld et al., 1989). As sulphate is not the only condensing species, the contribution of other secondary material in the growth rate has been taken into account, dividing the growth rate by the fraction of sulphate observed in the aerosol (see Fig. 2). The resulting $\tau_{V_i,\mathrm{cond}}$ can be interpreted as the time needed to produce in the particular compartment the amount of aerosol volume observed in the compartment.

Appendix B

AERO3 is a box model and simulates the aerosol dynamics of three particle populations: pure H_2SO_4–H_2O particles, pure soot particles, and mixed H_2SO_4–H_2O–soot particles. It allows for the internal mixing of the particles by coagulation, condensation, nucleation and in-cloud SO_2 oxidation.

In the model, sulphuric acid is formed from the gas phase by oxidation of SO_2 with OH radicals and can nucleate with water vapour forming H_2SO_4–H_2O droplets, or condense on aerosol particles. The nucleation of H_2O–H_2SO_4 droplets is treated using a parameterization of the homogeneous nucleation rates (Kulmala et al., 1998).

For relative humidity below 100% a H_2O–H_2SO_4 droplet can be considered to be in equilibrium with water vapour. Therefore, the equilibrium of the droplets may be described by the generalized Kelvin equation (Raes et al., 1992). For condensational growth both kinetic and continuum regimes are considered (Fuchs, 1964). Dry deposition is parameterized using a general correlation for particle deposition from turbulent gas flows to completely rough surfaces (Schack et al., 1985).

The H_2SO_4–H_2O and soot particles are assumed to be spheres. Their geometrical diameter is discretized using $D_{\mathrm{p,n}} = 0.002 \times 10^{(n/10)}$ μm, where $n = 0, 45$, corresponding to a range from 0.002 μm ($n = 0$) to 63 μm ($n = 45$). The mixed particles are assumed to consist of an insoluble (soot) core surrounded by a soluble (H_2SO_4–H_2O) shell. Their size is are discretisized into 46×46 classes, one dimension for the particle size and one dimension for the size of the insoluble core (Strom et al., 1992). Since the model cannot resolve particles with a water-soluble fraction less than 10%, the corresponding "less hygroscopic" particles have been assimilated into the insoluble population.

The evolution of particle number concentration is described by a system of coupled non-linear equations, one equation for each class (Vignati, 1999). The system of equations is solved using the Euler Backward Iterative method.

To describe the activation process, its assumed that all sulphuric acid is neutralized to ammonium sulphate and the Kohler equations extended to account for an insoluble core are applied (Seinfeld and Pandis, 1998).

Appendix C

The M^3 (Multi-Modal Model) model (Wilson and Raes, 1996) simulates the evolution of a sulphuric acid-water aerosol population, as three log-normally distributed modes (nucleation, Aitken and accumulation), with prescribed standard deviations, but varying number and mass (and therefore mean diameter).

The model simulates the competing processes of nucleation of new particles and condensation of gas-phase sulphate onto existing particles, together with coagulational growth of existing particles, cloud processing and dry and wet removal. M^3 has been compared with the full sectional aerosol model AERO2 (Raes et al., 1992) for a sample of 64 representative boundary layer cases, extracted at random from a climatological sulphur cycle model (Langner and Rodhe, 1991). The 24 h average total aerosol number concentrations and accumulation mode number concentrations predicted by the two models are shown in Fig. 7. The 24 h averages of the accumulation mode number concentrations predicted by M^3 are well within a factor of two of those predicted by AERO2.

In reality, sulphate is only one component of the aerosol burden. Therefore in implementing the M^3 model in the global off-line chemical transport model TM2, it is coupled to a model of the atmospheric black carbon cycle, and a static sea salt burden model. The following key assumptions are made:

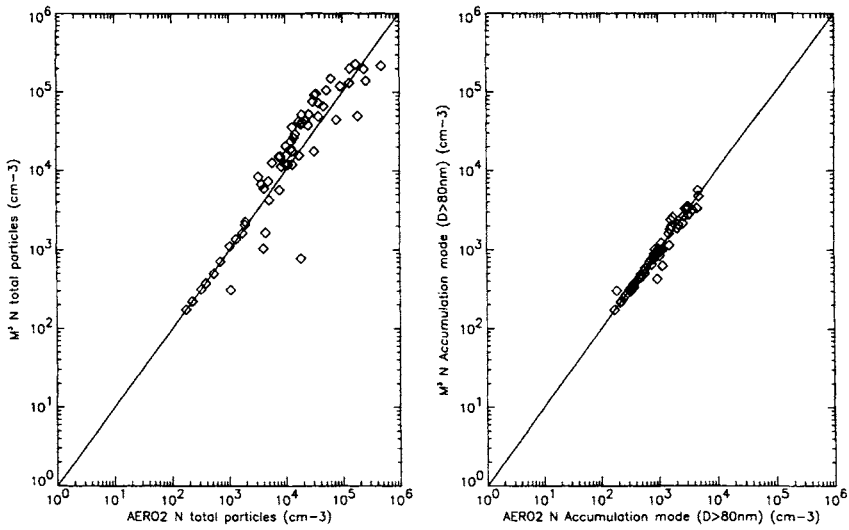

Figure 7. Comparison of the total number concentration and the number of accumulation mode particles calculated by the full sectional model AERO2 (Raes et al., 1992) and the simplified modal model M^3 (Wilson and Raes, 1996).

- Emissions of fossil fuel black carbon are assumed to be purely insoluble, and hence not subject to wet deposition. They age to a mixed and wet depositable aerosol through condensation of H_2SO_4.
- Biomass burning black carbon is a similar condensation sink, but its ageing, which is arbitrarily assumed to be 2.5% of mass per hour is independent of the sulphate condensed, as the co-emitted organic compounds are most likely to perform the ageing role rather than sulphate.

Details on the transport model and the emissions are given in Table 5.

References

Adams, P.J., Seinfeld, J.H., Koch, D.M., 1999. Global concentrations of tropospheric sulphate, nitrate, and ammonium simulated in a general circulation model. Journal of Geophysical Research 104, 13791–13823.

Aitken, J., 1888. On the number of dust particles in the atmosphere. Nature 37, 428–430.

Ammann, M., Kalberer, M., Jost, D.T., Tobler, L., Rossler, E., Piguet, D., Gaggeler, H.W., Baltensperger, U., 1998. Heterogeneous production of nitrous acid on soot in polluted air masses. Nature 395, 157–160.

Andronache, C., Chameides, W.L., Davis, D.D., Anderson, B.E., Pueschel, R.F., Bandy, A.R., Thornton, D.C., Talbot, R.W., Kasibhatla, P., Kiang, C.S., 1997. Gas-to-particle conversion of tropospheric sulphur as estimated from observations in the western North Pacific during PEM-West B. Journal of Geophysical Research 102, 28511–28538.

Ayers, G.P., Ivey, J.P., Gillet, R.W., 1991. Coherence between seasonal cycles of dimethyl sulphide, methanesulphonate and sulphate in marine air. Nature 349, 404–406.

Bates, T.S., Kapustin, V.N., Quinn, P.K., Covert, D.S., Coffman, D.J., Mari, C., Durkee, P.A., De Bruyn, W.J., Saltzman, E.S., 1998. Processes controlling the distribution of aerosol particles in the lower marine boundary layer during the First Aerosol Characterization Experiment (ACE 1). Journal of Geophysical Research 103, 16369–16383.

Bates, T.S., Cline, J.D., Gammon, R.H., Kelly-Hansen, S.R., 1987. Regional and seasonal variation in the flux of oceanic dimethylsulphide to the atmosphere. Journal of Geophysical Research 92, 2930–2938.

Blanchard, D.C., Woodcock, A.H., 1980. The production concentration and vertical distribution of the sea-salt aerosol. Annales of the New York Academy of Sciences 338, 330–347.

Boers, R., Ayers, G.P., Gras, J.L., 1994. Coherence between seasonal variation in satellite-derived cloud optical depth and boundary layer CCN concentrations at a mid-latitude Southern Hemisphere station. Tellus 46B, 123–131.

Calhoun, J.A., Bates, T.S., Charlson, R.J., 1991. Sulphur isotope measurements of submicrometer sulphate aerosol particles over the Pacific Ocean. Geophysical Research Letters 18, 1877–1880.

Capaldo, K.P., Kasibhatla, P., Pandis, S.N., 1999. Is aerosol production within the remote boundary layer sufficient to maintain observed concentrations? Journal of Geophysical Research 104, 3483–3500.

Cerveny, R.S., Balling, R.C., Jr., 1998. Weekly cycles of air pollutants, precipitation and tropical cyclones in the coastal NW Atlantic region. Nature 394, 561–663.

Charlson, R.J., Langner, J., Rodhe, H., Leovy, C.B., Warren, S.G., 1991. Perturbation of the nothern hemisphere radiative balance by backscattering from anthropogenic sulphate aerosols. Tellus 43AB, 152–163.

Charlson, R.J., Lovelock, J.E., Andreae, M.O., Warren, S.G., 1987. Oceanic phytoplankton, atmospheric sulphur, cloud albedo and climate. Nature 326, 655–661.

Chatfield, R.B., Crutzen, P.J., 1984. Sulphur dioxide in remote oceanic air: cloud transport of reactive precursors. Journal of Geophysical Research 89, 7111–7132.

Chin, M., Jacob, D., 1996. Anthropogenic and natural contributions to tropospheric sulphate: a global model analysis. Journal of Geophysical Research 101, 18691–18699.

Christoffersen, T.S., Hjorth, J., Horie, O., Jensen, N.R., Kotzias, D., Molander, L.L., Neeb, P., Ruppert, L., Winterhalter, R., Virkkula, A., Wirtz, K., Larsen, B., 1998. cis-Pinic acid, a possible precursor for organic aerosol formation from ozonolysis of alpha-pinene. Atmospheric Environment 32, 1657–1661.

Chuang, P.Y., Collins, D.R., Pawlowska, H., Snider, J.R., Jonsson, H.H., Brenguier, J.L., Flagan, R.C., Seinfeld, J.H., 2000. CCN measurements during ACE-2 and their relationship to cloud microphysical properties. Tellus 52B, 843–867.

Clarke, A.D., 1993. Atmospheric nuclei in the Pacific midtroposphere: their nature, concentration, and evolution. Journal of Geophysical Research 98, 20633–20647.

Clarke, A.D., 1992. Atmospheric nuclei in the remote free-troposphere. Journal of Atmospheric Chemistry 14, 479–488.

Clarke, A.D., Davis, D., Kapustin, V.N., Eisele, F., Chen, G., Paluch, I., Lenschow, D., Bandy, A.R., Thornton, D., Moore, K., Mauldin, L., Tanner, D., Litchy, M., Carroll, M.A., Collins, J., Albercook, G., 1998a. Particle nucleation in the tropical boundary layer and its coupling to marine sulphur sources. Science 282, 89–92.

Clarke, A.D., Porter, J.N., Valero, F.P.J., Pilewskie, P., 1996a. Vertical profiles, aerosol microphysics, and optical closure during ASTEX: measured and modeled column optical properties. Journal of Geophysical Research 101, 4443–4453.

Clarke, A.D., Uehara, T., Porter, J.N., 1996b. Lagrangian evolution of an aerosol column during the Atlantic Stratocumulus Transition Experiment. Journal of Geophysical Research 101, 4351–4362.

Clarke, A.D., Kapustin, V.N., Eisele, F.L., Weber, R.J., McMurry, P.H., 1999. Particle production near marine clouds: sulphuric acid and predictions from classical binary nucleation. Geophysical Research Letters 26, 2425–2428.

Clarke, A.D., Varner, J.L., Eisele, F., Mauldin, R.L., Tanner, D., Litchy, M., 1998b. Particle production in the remote marine atmosphere: cloud outflow and subsidence during ACE-1. Journal of Geophysical Research 103, 16397–16409.

Coffman, D.J., Hegg, D.A., 1995. A preliminary study of the effect of ammonia on particle nucleation in the marine boundary layer. Journal of Geophysical Research 100, 7147–7160.

Cooke, W., Wilson, J.N., 1996. A global black carbon aerosol model. Journal of Geophysical Research 101, 19395–19409.

Covert, D.S., Kapustin, V.N., Quinn, P.K., Bates, T.S., 1992. New particle formation in the marine boundary layer. Journal of Geophysical Research 92, 20581–20589.

Covert, D.S., Kapustin, V.N., Bates, T.S., Quinn, P.K., 1996. Physical properties of marine boundary layer aerosol particles of the Mid Pacific in relation to sources and meteorological transport. Journal of Geophysical Research 101, 6919–6930.

Dürbeck, T., Gerz, T., 1996. Dispersion of aircraft exhausts in the free atmosphere. Journal of Geophysical Research 101 (20), 26007–26015.

Easter, R.C., Peters, L.K., 1994. Binary homogeneous nucleation: temperature and relative humidity fluctuations, nonlinearity, and aspects of new particle production in the atmosphere. Journal of Applied Meteorology 33, 775–784.

Facchini, M.-C., Mircea, M., Fuzzi, S., Charlson, R.J., 1999. Cloud albedo enhancement by surface-active organic solutes in growing droplets. Nature 401, 257–259.

Feichter, J., Crutzen, P.J., 1990. Parameterization of vertical tracer transport due to deep cumulus convection in a global transport model and evaluation with radon measurements. Tellus 42B, 100–117.

Ferek, R.J., Chatfield, R.B., Andreae, M.O., 1986. Vertical distribution of dimethylsulphide in the marine atmosphere. Nature 320, 514–516.

Friedlander, S.K., 1977. Smoke, Dust and Haze: Fundamentals of Aerosol Behaviour. Wiley, New York.

Fuchs, N., 1964. The Mechanics of Aerosols. Pergamon, New York.

Gage, K.S., McAfee, J.R., Carter, D.A., Ecklund, W.L., Riddle, A.C., Reid, G.C., Balsley, B.B., 1991. Long-term mean vertical motion over the tropical pacific: wind-profiling doppler radar measurements. Science 254, 1771–1773.

Glasius, M., Lahaniati, M., Calogirou, A., Di Bella, D., Jensen, N.R., Hjorth, J., Kotzias, D., Larsen, B.R., 1999. Carboxilic acids in secondary aerosols from oxidation of cyclic monoterpenes by ozone. Environmental Science and Technology, in press.

Gong, S.L., Barrie, L.A., Blanchet, J.-P., 1997. Modeling sea-salt aerosols in the atmosphere 1. Model development. Journal of Geophysical Research 102, 3805–3818.

Griffin, R.J., Dabdub, D., Cocker III, D.R., Seinfeld, J.H., 1999a. Estimate of global atmospheric organic aerosol from oxidation of biogenic hydrocarbons. Geophysical Research Letters 26, 2721–2724.

Griffin, R.J., Cocker III, D.R., Flagan, R.C., Seinfeld, J.H., 1999b. Organic aerosol formation from the oxidation of biogenic hydrocarbons. Journal of Geophysical Research 104, 3555–3567.

Hamill, P., Turco, R.P., Kiang, C.S., Toon, O.B., Whitten, R.C., 1982. An analysis of various nucleation mechanisms for sulphate particles in the stratosphere. Journal of Aerosol Science 13, 561–585.

Hegg, D.A., Covert, D.S., Kapustin, V.N., 1992. Modeling case of particle nucleation in the marine boundary layer. Journal of Geophysical Research 97, 9851–9857.

Hegg, D.A., Radke, L.F., Hobbs, P.V., 1990. Particle production associated with marine clouds. Journal of Geophysical Research 95, 13917–13925.

Heimann, M., Monfray, P., Polian, G., 1990. Modeling the long-range transport of Rn-222 to subantarctic and antarctic areas. Tellus 42B, 83–99.

Heintzenberg, J., 1989. Fine particles in the global troposphere: a review. Tellus 41B, 149–160.

Heintzenberg, J., Covert, D.S., 1990. On the distribution of physical and chemical particle properties in the atmospheric aerosol. Journal of Atmospheric Chemistry 10, 383–397.

Heintzenberg, J., Covert, D.C., Van Dingenen R., 2000. Size distribution and chemical composition of marine aerosols: a compilation and review. Tellus, in press.

Hoppel, W.A., Frick, F.M., Larson, R.E., 1986. Effect of nonprecipitating clouds on the aerosol size distribution in the marine boundary layer. Geophysical Research Letters 13, 125–128.

Hoppel, W.A., Frick, G.M., Fitzgerald, J.W., Wattle, B.J., 1994a. A cloud chamber study of the effect that nonprecipitating water clouds have on the aerosol size distribution. Aerosol Science and Technology 20, 1–30.

Hoppel, W.A., Frick, G.M., Fitzgerald, J.W., Larson, R.E., 1994b. Marine boundary layer measurements of new particle formation and the effects nonprecipitating clouds have on aerosol size distribution. Journal of Geophysical Research 99, 14443–14459.

Hoppel, W.A., Fitzgerald, J.W., Frick, G.M., Larson, R.E., 1990. Aerosol size distributions and optical properties found in the marine boundary layer over the Atlantic Ocean. Journal of Geophysical Research 95, 3659–3686.

Jacob, D.J., Heikes, B.G., Fan, S.-M., Logan, J.A., Mauzerall, D.L., Bradshaw, J.D., Singh, H.B., Gregory, G.L., Talbot, R.W., Blake, D.E., Sachse, G.W., 1996. Origin of ozone and NO_x in the tropical troposphere: a photochemical analysis of aircraft observations over the South Atlantic basin. Journal of Geophysical Research 101, 24235–24250.

Jaenicke, R., 1988. Aerosol physics and chemistry. In: Landolt-Bornstein, Vol. 4. Springer, Berlin, pp. 391–457.

Jaecker-Voirol, A., Mirabel, P., 1989. Heteromolecular nucleation in the sulphuric acid-water system. Atmospheric Environment 23, 2053–2057.

Johnson, D., Osborne, S., Wood, R., Suhre, K., Johnson, R., Businger, S., Quinn, P.K., Wiedensohler, A., Durkee, P.A., Russell, L.M., Andreae, M.O., O'Dowd, C., Noone, K.J., Bandy, B., Rudolph, J., Rapsomanikis, S., 2000. An overview of the Lagrangian experiments undertaken during the North Atlantic regional aerosol characterization experiment (ACE-2). Tellus 52B, 290–320.

Katoshevski, D., Nenes, A., Seinfeld, J.H., 1999. A study of processes governing the maintenance of aerosols in the marine boundary layer. Journal of Aerosol Science 30, 503–532.

Koch, D.M., Jacob, D., Tegen, I., Rind, D., Chin, M., 1999. Tropospheric sulphur simulation and sulphate direct radiative forcing in the GISS GCM. Journal of Geophysical Research 104, 23799–23822.

Kohler, H., 1936. The nucleus in and the growth of hygroscopic droplets. Transactions of the Faraday Society 32, 1152.

Korhonen, P., Kulmala, M., Laaksonen, A., Viisanen, Y., McGraw, R., Seinfeld, J.H., 1999. Ternary nucleation of H_2SO_4, NH_3, and H_2O in the atmosphere. Journal of Geophysical Research 104, 26349–26353.

Kulmala, M., Laaksonen, A., Charlson, R.J., Korhonen, P., 1997. Clouds without supersaturation. Nature 388, 336.

Kulmala, M., Laaksonen, A., Pirjola, L., 1998. Parameterizations for sulphuric acid/water nucleation rates. Journal of Geophysical Research 103, 8301–8308.

Kulmala, M., Pirjola, L., Makela, J.M., 2000. Stable sulphate clusters as a source of new atmospheric particles. Nature 404, 66–69.

Lai, F.S., Friedlander, S.K., Pich, J., Hidy, G.M., 1972. The self-preserving particle size distribution for Brownian coagulation in the free-molecular regime. Journal of Colloid and Interface Science 39, 395–405.

Langner, J., Rodhe, H., 1991. A global three-dimensional model of the tropospheric sulphur cycle. Journal of Atmospheric Chemistry 13, 225–263.

Lelieveld, J., Crutzen, P.J., 1994. Role of deep cloud convection in the ozone budget of the troposphere. Science 264, 1759–1761.

Lelieveld, J., Crutzen, P.J., Rodhe, H., 1989. Zonal average cloud characteristics for global atmospheric chemistry modelling. Report CM-76, Department of Meteorology University of Stockholm, Stockholm, Sweden.

Li, Z., Williams, A.L., Rood, M.J., 1998. Influence of soluble surfactant properties on the activation of aerosol particles containing inorganic solute. Journal of Atmospheric Sciences 55, 1859–1865.

Liousse, C., Penner, J.E., Chuang, C., Walton, J.J., Eddleman, H., Cachier, H., 1996. A global three-dimensional model study of carbonaceous aerosols. Journal of Geophysical Research 101, 19411–19432.

Maring, H., Savoie, D.L., Izaguirre, M.A., McCormick C., Arimoto, R., Prospero, J.M., Pilinis, C., 2000. Aerosol physical and optical properties and their relation to aerosol composition in the free troposphere at Izaña, Tenerife, Canary Islands during July 1995. Journal of Geophysical Research 105, 14677–14700.

Mason, B.J., 1971. The Physics of Clouds. Clarendon Press, Oxford.

Mauldin III, R.L., Madronich, S., Flocke, S.J., Eisele, F.L., Frost, G.J., Prevot, A.S.H., 1997. New insights on OH: measurements around and in clouds. Geophysical Research Letters 24, 3033–3036.

Meng, Z., Seinfeld, J.H., 1996. Time scales to achieve atmospheric gas-aerosol equilibrium for volatile species. Atmospheric Environment 30, 2889–2900.

Murphy, D.M., Anderson, J.R., Quinn, P.K., McInnes, L.M., Brechtel, F.J., Kreidenweiss, S.M., Middlebrook, A.M., Posfai, M., Thomson, D.S., Buseck, P.R., 1998a. Influence of sea-salt on aerosol radiative properties in the Southern Ocean marine boundary layer. Nature 392, 62–65.

Murphy, D.M., Thomson, D.S., Mahoney, M.J., 1998b. In situ measurements of organics, meteoritic material, mercury, and other elements in aerosols at 5 to 19 kilometers. Science 282, 1664–1669.

Newell, R.E., 1979. Climate and the ocean. American Scientist 67, 405–416.

Newell, R.E., Zhu, Y., Browell, E.V., Read, W.G., Waters, J.W., 1996. Walker circulation and tropical upper tropospheric water vapor. Journal of Geophysical Research 101, 1961–1974.

Newell, R.E., Thouret, V., Cho, J.Y.N., Stoller, P., Marenco, A., Smit, H.G., 1999. Ubiquity of quasi-horizontal layers in the tropophere. Nature 398, 316–319.

Nilsson, E.D., Kulmala, M., 1998. The potential for atmospheric mixing processes to enhance the binary nucleation rate. Journal of Geophysical Research 103, 1381–1389.

Novakov, T., Penner, J.E., 1993. Large contribution of organic aerosols to cloud-condensation-nuclei concentrations. Nature 365, 823–826.

Novakov, T., Hegg, D.A., Hobbs, P.V., 1997. Airborne measurements of carbonaceous aerosols on the East Coast of the United States. Journal of Geophysical Research 102, 30023–30030.

O'Dowd, C.D., Smith, M.H., 1993. Physicochemical properties of aerosols over the Northeast Atlantic: evidence for wind-speed-related sub-micron sea-salt aerosol production. Journal of Geophysical Research 98, 1137–1149.

Odum, J.R., Hoffman, T., Bowman, F., Collins, D., Flagan, R.C., Seinfeld, J.H., 1996. Gas/Particle partitioning and secondary aerosol yields. Environmental Science and Technology 30, 2580–2585.

Oort, A.H., 1983. Global atmospheric circulation statistics 1958–1973. NOAA Professional Paper No 14. US Government Printing Office, Washington, DC.

Ostrom, E., Noone, K.J., 2000. Vertical profiles of aerosol scattering and absorption measured in-situ during the North Atlantic aerosol characterization experiment (ACE-2). Tellus 52B, 526–545.

Pawlowska, H., Brenguier, J.-L., 2000. Microphysical properties of stratocumulus clouds during ACE-2. Tellus 52B, 868–887.

Perry, K.D., Hobbs, P.V., 1994. Further evidence for particle nucleation in clean air adjacent to marine cumulus clouds. Journal of Geophysical Research 99, 22803–22818.

Pruppacher, H.R., Klett, J.D., 1980. Microphysics of Clouds and Precipitation. Reidel, Dordrecht.

Putaud, J.-P., Van Dingenen, R., Mangoni, M., Virkkula, A., Raes, F., Maring, H., Prospero, J., Swietlicki, E., Berg, O., Hillamo, R., Makela, T., 2000. Chemical mass closure and assessment of the origin of the sub-micron aerosol in the marine boundary layer and the free troposphere at Tenerife during ACE-2. Tellus 52B, 141–168.

Raes, F., Wilson, J., Van Dingenen, R., 1995. Aerosol dynamics and its implication for the global aerosol climatology. In: Charson, R.J., Heintzenberg, J. (Eds.), Aerosol Forcing of Climate. Wiley, New York.

Raes, F., Van Dingenen, R., 1992. Simulations of condensation and cloud condensation nuclei from biogenic SO_2 in the remote marine boundary layer. Journal of Geophysical Research 97, 12901–12912.

Raes, F., Van Dingenen, R., 1995. Comment on "The relationship between DMS flux and CCN concentrations in remote marine regions" by S.N. Pandis, L.M. Russell, and J.H. Seinfeld. Journal of Geophysical Research 100, 14355–14356.

Raes, F., 1995. Entrainment of free tropospheric aerosols as a regulating mechanism for cloud condensation nuclei in the remote marine boundary layer. Journal of Geophysical Research 100, 2893–2903.

Raes, F., Janssens, A., Van Dingenen, R., 1986. The role of ion-induced aerosol formation in the lower atmosphere. Journal of Aerosol Science 17, 466–470.

Raes, F., Van Dingenen, R., Saltelli, A., 1992. Modelling the dynamics of H_2SO_4–H_2O aerosols with $AERO_2$: model description, uncertainty analysis and experimental validation. Journal of Aerosol Science 23, 759–771.

Raes, F., Van Dingenen, R., Cuevas, E., Van Velthoven, P.F.J., Prospero, J.M., 1997. Observations of aerosols in the free troposphere and marine boundary layer of the subtropical Northeast Atlantic: discussion of processes determining their size distribution. Journal of Geophysical Research 102, 21315–21328.

Raes, F., Van Dingenen, R., Wilson, J., Saltelli, A., 1993. Cloud condensation nuclei from dimethyl sulphide in the natural marine boundary layer: remote vs. in-situ production. In: Restelli, G., Angeletti, G. (Eds.), DMS: Ocean, Atmosphere and Climate. Kluwer Academic Publisher, Dordrecht, pp. 311–322.

Rodhe, H., 1983. Precipitation scavenging and tropospheric mixing. In: Pruppacher et al. (Eds.), Precipitation Scavenging, Dry Deposition, and Resuspension, pp. 719–728.

Rosenfeld, D., 1999. TRMM observed first direct evidence of smoke from forest fires inhibiting rainfall. Geophysical Research Letters 26, 3105–3108.

Russell, L.M., Pandis, S.N., Seinfeld, J.H., 1994. Aerosol production and growth in the marine boundary layer. Journal of Geophysical Research 99, 20989–21003.

Saxena, P., Hildemann, L.M., McMurry, P.H., Seinfeld, J.H., 1995. Organics alter hygroscopic behaviour of atmospheric particles. Journal of Geophysical Research 100, 18755–18770.

Saxena, P., Hildemann, L., 1996. Water-soluble organics in atmospheric particles: a critical review of the literature and application of thermodynamics to identify candidate compounds. Journal of Atmospheric Chemistry 24, 57–109.

Schack, C.J., Pratsinis, S.E., Friedlander, S.K., 1985. A general correlation for deposition of suspended particles from turbulent gases to completely rough surfaces. Atmospheric Environment 19, 953–960.

Schulz, M., Balkanski, Y.J., Guelle, W., Dulac, F., 1998. Role of aerosol size distribution and source location in a three-dimensional simulation of a Saharan dust episode tested against satellite-derived optical thickness. Journal of Geophysical Research 103, 10579–10592.

Schwikowski, M., Seibert, P., Baltensberger, U., Gaggeler, H.W., 1995. A study of an outstanding Saharan dust event at the high-alpine site Jungfraujoch. Switzerland, Atmospheric Environment 29, 1829–1842.

Seinfeld, J.H., Pandis, S.N., 1998. Atmospheric Chemistry and Physics: from Air Pollution to Climate Change. Wiley, New York.

Shulman, M.L., Jacobson, M.C., Charson, R.J., Synovec, R.E., Young, T.E., 1996. Dissolution behaviour and surface tension effects of organic compounds in nucleating cloud droplets. Geophysical Research Letters 23, 277–280.

Sprengard-Eichel, C., Krämer, M., Schütz, L., 1998. Soluble and insoluble fractions of urban, continental and marine aerosol. Journal of Aerosol Science 29, S175–S176.

Strom, J., Okada, K., Heintzenberg, J., 1992. On the state of mixing of particles due to Brownian coagulation. Journal of Aerosol Science 23, 467–480.

Svenningsson, B., Hansson, H.-C., Wiedensohler, A., Noone, K.J., Ogren, J., Hallberg, A., Colville, R., 1994. Hygroscopic growth of aerosol particles and its influence on nucleation scavenging in cloud: experimental results from Kleiner Feldberg. Journal of Atmospheric Chemistry 19, 129–152.

Swietlicki, E., Zhou, J., Covert, D.S., Hameri, K., Busch, B., Vakeva, M., Dusek, U., Berg, O.H., Wiedensohler, A., Aalto, P., Makela, J., Martinsson, B.G., Papaspiropoulos, G., Mentes, B., Frank, G., Stratmann, F., 2000. Hygroscopic properties of aerosol particles in the north-eastern Atlantic during ACE-2. Tellus 52B, 201–227.

Tegen, I., Hollrig, P., Chin, M., Fung, I., Jacob, D., Penner, J., 1997. Contribution of different aerosol species to the global aerosol extinction optical thickness: estimates from model results. Journal of Geophysical Research 102, 23895–23915.

Thornton, D.C., Bandy, A.R., Blomquist, B.W., Bradshaw, J.D., Blake, D.R., 1997. Vertical transport of sulphur dioxide and dimethyl sulphide in deep convection and its role in new particle formation. Journal of Geophysical Research 102, 28501–28509.

Turco, R.P., Zhao, J.-X., Yu, F., 1998. A new source of tropospheric aerosols: ion-ion recombination. Geophysical Research Letters 25, 635–638.

Van Dingenen, R., Raes, F., Jensen, N.R., 1995. Evidence for anthropogenic impact on number concentration and sulphate content of cloud-processed aerosol particles over the North-Atlantic. Journal of Geophysical Research 100, 21057–21067.

Van Dingenen, R., Raes, F., Putaud, J.-P., Virkkula, A., Mangoni, M., 1999. Processes determining the relationship between aerosol number and non-seasalt sulphate mass concentrations in the clean and perturbed marine boundary layer. Journal of Geophysical Research 104, 8027–8038.

Van Dingenen, R., Virkkula, A.O., Raes, F., Bates, T.S., Wiedensohler, A., 2000. A simple non-linear analytical relationship between aerosol accumulation number and sub-micron volume, explaining their observed ratio in the clean and polluted marine boundary layer. Tellus 52B, 439–451.

Vignati, E., 1999. Modelling interactions between aerosols and gaseous compounds in the polluted marine atmosphere. Ph.D. Thesis, RISOE National Laboratory, Report No. Riso-R-1163(EN), p. 133.

Virkkula, A., Van Dingenen, R., Raes, F., Hjorth, J., 1999. Hygroscopic properties of aerosol formed by oxidation of limonene, alpha-pinene and beta-pinene. Journal of Geophysical Research 104, 3569–3579.

Vogt, R., Crutzen, P.J., Sander, R., 1996. A mechanism for halogen release from sea-salt aerosol in the remote marine boundary layer. Nature 383, 327–330.

Wang, C., Crutzen, P.J., Ramanathan, V., Williams, S.F., 1995. The role of a deep convective storm over the tropical Pacific Ocean in the redistribution of atmospheric chemical species. Journal of Geophysical Research 100, 11509–11516.

Wang, P.-H., Rind, D., Trepte, C.R., Kent, G.S., Yue, G.K., Skeens, K.M., 1998. An empirical model study of the tropospheric meridional circulation based on SAGE II observations. Journal of Geophysical Research 103, 13801–13818.

Weber, R.J., Marti, J.J., McMurry, P.H., Eisele, F.L., Tanner, D.J., Jefferson, A., 1996. Measured atmospheric new particle formation rates: implications for nucleation mechanisms. Chemical Engineering Communications 151, 53–64.

Weber, R.J., McMurry, P.H., Eisele, F.L., Mauldin, L., Tanner, D., 1998. Rapid growth of freshly formed nanoparticles in the remote troposphere. Journal of Aerosol Science 29, S179–S180.

Went, F.W., 1960. Blue hazes in the atmosphere. Nature 187, 641–643.

Wexler, A.S., Seinfeld, J.H., 1990. The distribution of ammonium salts among a size and composition dispersed aerosol. Atmospheric Environment 24A, 1231–1246.

Whitby, K.T., 1978. The physical characteristics of sulphur aerosols. Atmospheric Environment 12, 135–159.

Wilson, J.J.N., Raes, F., 1996. M3 a multi modal model for aerosol dynamics. In: Kulmala, D., Wagner, D. (Eds.), Proceedings of the 14th International Conference on Nucleation and Atmospheric Aerosols. Pergamon, Oxford, pp. 458–461.

Wu, Z., Newell, R.N., Zhu, Y., Anderson, B.E., Browell, E.V., Gregory, G.L., Sachse, G.W., Collins, Jr., J.E., 1997. Atmospheric layers measured from the NASA DC-8 during PEM-West B and comparison with PEM-West A. Journal of Geophysical Research 102, 28353–28365.

Yu, J., Cocker, D.R., Griffin, R.J., Flagan, R.C., Seinfeld, J.H., 1999. Gas-phase ozone oxidation of monoterpenes: gaseous and particulate products. Journal of Atmospheric Chemistry 34, 207–258.

Zhang, Y., Seigneur, C., Seinfeld, J.H., Jacobson, M., Clegg, S.L., Binkowski, F.S., 2000. A comparative review of inorganic aerosol thermodynamics equilibrium modules: similarities, differences, and their likely causes. Atmospheric Environment 34, 117–137.

Zhang, X.Q., McMurry, P.H., Hering, S.V., Casuccio, G.S., 1993. Mixing characteristics and water content of sub-micron aerosols measured in Los Angeles and at the Grand Canyon. Atmospheric Environment 27A, 1593–1607.

Zimmermann, P.H., 1984. Ein dreidimensionales numerisches Transportmodell fur atmospharische Spurenstoffe. Thesis, Univeristy of Mainz, FRG.